

Kinetics of Manganese Adsorption, Desorption and Oxidation in Coastal Marine Sediments

by

Dominique Richard

A thesis submitted to McGill University in partial fulfilment of the
requirements of the degree of Master of Science

Earth and Planetary Sciences
McGill University
Montreal, Canada
June 2011

© Dominique Richard, 2011

To my parents, Jo-Anne and Jean Richard,
my husband Guillaume Joyal and our future baby girl

À mes parents, Jo-Anne et Jean Richard,
à mon amour, Guillaume Joyal et à « Melon »

Contributions of authors

This thesis is the result of my M.Sc. research project in the Department of Earth and Planetary Sciences at McGill University. It comprises three chapters, one of which is a scientific manuscript while the two others are a general introduction and conclusion. The subject of this thesis was proposed by Professor Bjørn Sundby. Sample collection in the field was conducted by myself and Qiang Chen under the guidance of Professor Alfonso Mucci. All laboratory and analytical work for this thesis was completed by myself. Professors Bjørn Sundby and Alfonso Mucci provided guidance on the research methodology, advised me with the processing and interpretation of the data and contributed to the preparation of this thesis.

Acknowledgements

I am very grateful to Professor Bjørn Sundby for the funding provided for this research project and for the way he made things simple all the time. I would also like to thank the donors of the J.W. McConnell Memorial Fellowship, the Alexander A. McGregor fellowship and the Robert Wares Fellowship for the encouragement provided by their financial support.

Furthermore, I would like to express my sincere gratitude to the following people: my advisors, Professors Bjørn Sundby and Alfonso Mucci for their availability, support and guidance throughout the project, Glenna Keating and Isabelle Richer for their assistance in the geochemical laboratory, and Constance Guignard for her help with the management of supplies and her assistance in the low temperature geochemistry laboratory. In addition, I am grateful to all of my colleagues in the office who made it pleasant to work at McGill. Special thanks to Thais Lamana, Fatimah Sulu-Gambari, Qiang Chen and Stelly Lefort for their help and advice. Finally, I would like to thank Rénaud Belley, Gwen Chaillou and Philippe Archambault from l'UQAR for making my stay in Rismouski enjoyable and instructive.

Abstract

In organic-rich sediments with a thin oxidised surface layer, sediment resuspension by physical or biological processes may contribute to the manganese flux by exposing Mn(II)-laden anoxic sediment to the water column. The adsorbed Mn(II) can then be desorbed to the water column or sequestered by the solid phase upon oxidation to insoluble Mn(IV) oxides. Ultimately, the flux of Mn(II) to the water column depends on the relative rates of Mn(II) desorption and Mn(II) oxidation at the surface of sediment particles. First-order rate constants for adsorption, desorption and oxidation of Mn(II) in natural anoxic sediment were determined experimentally by monitoring dissolved manganese concentrations in sediment incubations. Adsorption and desorption reactions were initiated by mixing anoxic sediment and bottom water from the Lower St. Lawrence Estuary in closed reactors under anoxic conditions. Once sorption reactions reached a steady state, oxidation was initiated by introducing ambient air into the reactors. The kinetics of Mn(II) adsorption, desorption, and oxidation were fitted to first-order rate laws and the following first-order rate constants were obtained: $k_{ads}' = 7.0 \pm 3.4 \text{ h}^{-1}$, $k_{des}' = 12.7 \pm 3.3 \text{ h}^{-1}$, $k_{ox}' = 0.020 \pm 0.006 \text{ h}^{-1}$. According to our results, desorption occurs more rapidly than oxidation and allows dissolved manganese to be released upon exposure of reducing sediment to oxygenated bottom seawater.

Résumé

Dans un sédiment riche en matière organique et ayant un horizon oxydé mince, la mise en suspension de sédiments par des processus physiques ou biologiques pourrait contribuer au flux sortant de manganèse en exposant des sédiments anoxiques à la colonne d'eau. Le Mn(II) adsorbé aux particules sédimentaires peut être désorbé dans la colonne d'eau ou séquestré suite à son oxydation et à la formation d'oxydes de Mn(IV) insolubles. Le flux de Mn(II) vers la colonne d'eau dépend ultimement de la vitesse relative des réactions de désorption et d'oxydation à la surface de ces particules. Afin de déterminer si la mise en suspension de sédiments réduits contribue au flux sortant de manganèse, nous avons déterminé les constantes de vitesse de premier ordre pour les réactions d'adsorption, de désorption et d'oxydation du Mn(II) en suivant l'évolution des concentrations de manganèse dissout dans des suspensions de sédiments naturels. Les réactions d'adsorption et de désorption ont été initiées en mélangeant des sédiments anoxiques et de l'eau de fond provenant de l'estuaire maritime du Saint-Laurent dans des réacteurs fermés en absence d'oxygène. Lorsque les réactions de sorption ont atteint un état stationnaire, l'oxydation fut initiée en introduisant de l'air ambiant dans les réacteurs. Les cinétiques d'adsorption, de désorption et d'oxydation du Mn(II) ont été représentées par des cinétiques d'ordre 1 et les constantes de vitesse suivantes ont été obtenues : $k_{ads}' = 7.0 \pm 3.4 \text{ h}^{-1}$, $k_{des}' = 12.7 \pm 3.3 \text{ h}^{-1}$, $k_{ox}' = 0.020 \pm 0.006 \text{ h}^{-1}$. Selon nos résultats, la désorption du Mn(II) est plus rapide que son oxydation et contribuerait par conséquent au flux sortant de manganèse lors de la mise en suspension de sédiments réduits.

Table of contents

CHAPTER 1. INTRODUCTION AND LITERATURE REVIEW	10
1.1 INTRODUCTION	10
1.2 RATIONALE	12
1.3 LITERATURE REVIEW	13
1.3.1 <i>Manganese</i>	13
1.3.2 <i>Sediment resuspension</i>	15
1.3.3 <i>Manganese oxidation kinetics</i>	16
1.3.4 <i>Manganese sorption kinetics</i>	18
1.4 OBJECTIVES	19
1.5 REFERENCES	20
CHAPTER 2. KINETICS OF MANGANESE ADSORPTION, DESORPTION, AND OXIDATION IN COASTAL MARINE SEDIMENTS	28
2.1 INTRODUCTION	28
2.2 MATERIAL AND METHODS	31
2.2.1 <i>Environmental setting</i>	31
2.2.2 <i>Sediment characteristics</i>	32
2.2.3 <i>Sampling and storage</i>	33
2.2.4 <i>Sediment and porewater analyses</i>	34
2.2.5 <i>Slurry incubation experiments</i>	35
2.2.5.1 Adsorption and desorption experiments	36
2.2.5.2 Oxidation experiments	38
2.2.5.3 pH measurements	38
2.2.5.4 HEPES buffer	39
2.3 RESULTS AND DISCUSSION	39
2.3.1 <i>Desorption and adsorption experiments</i>	39
2.3.2 <i>Oxidation experiments</i>	41
2.3.3 <i>Adsorption and desorption kinetics</i>	42
2.3.4 <i>Oxidation kinetics</i>	44
2.3.5 <i>Desorption kinetics vs. oxidation kinetics</i>	46
2.3.6 <i>Caveat</i>	48
2.4 SUMMARY	49
2.5 REFERENCES	51
CHAPTER 3. FINAL REMARKS	78
3.1 RESEARCH SUMMARY AND CONCLUSIONS	78
3.2 FINAL REMARKS AND RECOMMENDATIONS	79
3.3 FUTURE WORK	81
3.4 REFERENCES	83

Table of figures

Figure 1.1 – Fields of stability of dissolved species and solids phases of Mn as a function of pH and Eh at 25°C and 1 atm in the Mn-CO ₂ -H ₂ O system. Bicarbonate species concentration: 2 mg/L. Modified from Hem (1972).	27
Figure 2.1 – Map of the Lower St. Lawrence Estuary showing the position of Station 23.....	57
Figure 2.2 – A) Vertical distributions of reactive particulate Mn and Fe (μmol/g dry wt.) and total I (100 × μmol/g dry wt.) at Station 23. B) Vertical distributions of dissolved O ₂ , I(-I), Mn(II) and Fe(II) in sediment porewaters at Station 23 in μmol/L. The profiles were acquired with a solid-state gold/mercury amalgam microelectrode (Brendel and Luther, 1995). The detection limits for O ₂ , I(-I), Mn(II) and Fe(II) were 3 μmol/L, <0.2 μmol/L, and 5 μmol/L, respectively. Figures taken from Anschutz et al. (2000).....	58
Figure 2.3 – Schematic representation of the experimental reactor.	59
Figure 2.4 – Desorption experiments #4-5 (43 g/L), #8-9 (26 g/L) and #10-11 (43 g/L – HEPES 5 mM). Panel A shows the evolution of the dissolved Mn concentration during the course of the experiments. Panel B shows the temporal evolution of dissolved Mn concentration normalised to the dry weight of solid sediment. This ratio is obtained by dividing the concentration of dissolved Mn by the solid/solution ratio of the slurry and carries units of μmol g ⁻¹ dry sediment.....	60
Figure 2.5 – Adsorption experiments #6-7 (43 g/L) and #12-13 (43 g/L – HEPES 20 mM). Panel A shows the evolution of the dissolved Mn concentration during the course of the experiments. Panel B shows the temporal evolution of dissolved Mn concentration normalised to the dry weight of solid sediment. This ratio is obtained by dividing the concentration of dissolved Mn by the solid/solution ratio of the slurry and carries units of μmol g ⁻¹ dry sediment.....	61
Figure 2.6 – Oxidation experiments #6-7 (Ads), #12-13 (Ads –HEPES 20 mM), #4-5 (Des) and #10-11 (Des – HEPES 5 mM). Panel A shows the evolution of the dissolved Mn concentration during the course of the experiments. Panel B show the temporal evolution of pH during the course of the experiments. The solid/solution ratio was 43 g/L for all experiments.	62
Figure 2.7 – First-order kinetics plot based on the time evolution of dissolved Mn concentrations in slurries during desorption experiments. The first-order rate constant $k_{des}' = 0.21 \pm 0.06 \text{ min}^{-1}$ was obtained from the slope of the regression line for the combined experiments #4-5 (43 g/L), #8-9 (26 g/L) and #10-11 (43 g/L – HEPES 5 mM). Only data obtained during the initial 15 minutes of each experiment were used to calculate the regression (see text for justification). The uncertainty on the least squares regression represents the 95% confidence interval.	63

Figure 2.8 – First-order kinetics plot based on the time evolution of dissolved Mn concentrations in slurries during adsorption experiments. The first-order rate constant $k_{ads}' = 0.12 \pm 0.06 \text{ min}^{-1}$ was obtained from the slope of the regression line for the combined experiments #6-7 (43 g/L) and #12-13 (43 g/L – HEPES 20 mM). Only data obtained during the initial 7 minutes of each experiment were used to calculate the regression. The uncertainty on the least squares regression represents the 95% confidence interval.	64
Figure 2.9 – First-order kinetics plot based on the time evolution of dissolved Mn concentrations in slurries during oxidation experiments. The pseudo-first-order rate constant $k_{ox}' = 0.020 \pm 0.006 \text{ hours}^{-1}$ was obtained from the slope of the regression line for the combined experiments #6-7 (Ads), #12-13 (Ads – HEPES 20 mM), #4-5 (Des) and #10-11 (Des – HEPES 5 mM). Only data obtained in the initial 12 hours of each experiment were used to calculate the regression. The uncertainty on the least squares regression represents the 95% confidence interval.	65
Figure 2.10 – Simulation of the hypothetical temporal evolution of dissolved Mn(II) from competing desorption and oxidation reactions upon exposure of anoxic sediments to oxygenated waters at 25°C and pH _{sws} = 7.7. In this simulation, $R = k_{des}' ([Mn_{diss}]_{ss} - [Mn_{diss}]) - k_{ox}' [Mn_{diss}]$ (see Eq. 3a and Eq. 4), for which the analytical solution is : $[Mn_{diss}]_t = ([Mn_{diss}]_{ss} (1 - e^{-k_{des}'t})) - e^{-k_{ox}'t}$. In this simulation $[Mn_{diss}]_{ss} = 12.5 \text{ } \mu\text{mol/L}$ (the mean steady state value for desorption experiments #4-5 and #10-11 at a solid:solution ratio of 43 g/L).	66

List of tables

Table 2.1 - Characteristics of homogenised sediment recovered at Station -23 in July 2009	67
Table 2.2 - Characteristics and quantity of seawater and sediment used for the slurry incubation experiments	67
Table 2.3 – Desorption experiments #4-5, #8-9 and #10-11	68
Table 2.4 – Adsorption experiments #6-7 and #12-13	71
Table 2.5 – Oxidation experiments #4-5, #6-7, #10-11 and #12-13	73
Table 2.6 – Compilation of the Mn(II) first-order oxidation rate constants taken from the literature and measured in this study	77

Chapter 1. Introduction and literature review

1.1 Introduction

The microbially-mediated oxidation of organic matter in marine sediments reduces oxidants and releases metabolites and soluble metals to the porewaters. The principal oxidants (O_2 , NO_3^- , MnO_2 , Fe-oxides, SO_4^{2-} and CO_2) are consumed in a sequence of reactions determined by the free energy yield of the terminal electron transfer step (Froelich *et al.*, 1979; Gaillard *et al.*, 1989). The sequence begins with oxic respiration and is followed by denitrification, manganese oxide reduction, iron oxide reduction, sulphate reduction, and finally fermentation.

In environments receiving large amounts of organic matter, such as coastal sediments, the oxidant demand by the sediment can be high. Consequently, oxygen only penetrates a millimetres below the sediment surface, and reduction of iron and manganese oxides takes place near the sediment-water interface. A good example is the bottom sediment of the Lower St. Lawrence Estuary (LSLE). Here, a sharp color contrast, located typically less than 1 cm below the sediment-water interface, indicates the position of the oxic-anoxic boundary (Anschutz *et al.*, 2000). Above this boundary, Mn(IV) and Fe(III) (hydr)oxides are responsible for the brown coloration of the sediment. Below the boundary, many of these metal oxides are reduced and the sediment is grey. The reductive dissolution of

iron and manganese oxides releases soluble Mn(II) and Fe(II) to the porewaters, creating concentration gradients along which these metals can diffuse.

Manganese cycles across the oxic-anoxic boundary via burial of oxidised manganese below the boundary, reductive dissolution, upward diffusion across the boundary, and oxidation and re-precipitation in the oxic layer. This cycle enriches the oxic surface sediment in manganese at the expense of the anoxic subsurface sediment. In some coastal environments, mass balance considerations have shown that the subsurface solid phase manganese concentration, representing the manganese that is truly retained by the sediment, can be considerably lower than the manganese content of the particulate matter brought to the system by rivers. The difference is explained by a net export of manganese from the sediment to the overlying waters and out of the system (Sundby *et al.*, 1981; Trefry and Presley, 1982). For the Estuary and Gulf of St. Lawrence, Sundby *et al.* (1981) estimated that 5.0×10^9 g/yr of manganese, which is 50% more than the river input of dissolved manganese, escapes from the sediment and are exported to the open ocean in the suspended matter load.

A combination of several mechanisms may be responsible for the manganese flux from sediment to water column. These mechanisms include diffusion of dissolved manganese across the oxidised surface layer (McCaffrey *et al.*, 1980; Sundby *et al.*, 1981) and porewater advection by physical or biological processes (McCaffrey *et al.*, 1980; Burdige, 2006). Diffusion of dissolved manganese across the sediment-water interface is favoured by two factors: the slow oxidation kinetics of Mn(II) by oxygen and periodic excursions of the

manganese redox boundary towards the sediment-water interface (Sundby, 2006). Migration of redox boundaries in sediment occurs in response to persistent or episodic changes in the flux of degradable organic matter to the seafloor or variation of the concentration of dissolved oxygen in the overlying bottom water (Burdige, 1993). Evidence for a fluctuating Mn(II)/Mn(IV) redox boundary has been reported in many coastal sediments (e.g. Aller, 1994; Thamdrup *et al.*, 1994a; Gobeil *et al.*, 1997). In some cases, the manganese redox boundary may reach the sediment-water interface and allow dissolved manganese to escape directly to the water column (Sundby, 2006). Advection of anoxic sediment to the sediment-water interface by physical or biological processes may also lead to manganese release from the sediment (Schink and Guinasso, 1978; Saulnier and Mucci, 2000; Kalnejais *et al.*, 2010). As anoxic sediment is resuspended, manganese may be released to the water column by desorption from sediment particles. This mechanism, which has received little attention, is the subject of this thesis.

1.2 Rationale

In sedimentary environments with a thin oxidised surface layer, sediment resuspension by physical or biological processes brings anoxic sediment in direct contact with the water column. The contact between anoxic sediment and bottom water facilitates exchange of soluble sediment constituents with the water and can affect the burial efficiency of diagenetic reaction products (Aller *et al.*, 2001).

In the subsurface anoxic sediment, the Mn(II) that is produced by reductive dissolution of manganese oxides is in part adsorbed onto sediment particles and released to the porewater (Van der Zee *et al.*, 2001; Sundby, 2006). Pore water Mn(II) can diffuse upward, cross the oxic-anoxic boundary, and be oxidised and precipitated as an authigenic oxide in the oxic surface layer. Depending on the thickness of the oxic layer and the Mn(II) oxidation rate, all or part of the diffusing Mn(II) may be trapped before it can leave the surface layer. In contrast, advected anoxic sediment bypasses the oxic surface layer entirely, which allows dissolved and adsorbed Mn(II) to be exposed directly to the water column. Unlike the anoxic sediment porewater, the overlying water is typically oxygenated and nearly devoid of dissolved manganese (e.g. Yeats *et al.*, 1979). The sudden exposure of adsorbed Mn(II) to this water triggers two competing reactions: 1) oxidation of soluble Mn(II) to insoluble Mn(IV), and 2) desorption of Mn(II) which may escape the sediment and be released to the water column. The relative rates of these two competing reactions are not known, and it is *a priori* impossible to determine which reaction dominates.

1.3 Literature review

1.3.1 Manganese

Manganese is the eleventh most abundant constituent in the Earth's crust and the third most abundant transition metal (Taylor, 1964). It is an essential trace

nutrient for most living organisms and can be found in the lithosphere, the atmosphere, and the hydrosphere in the following oxidation states: Mn(II), Mn(III) and Mn(IV) (Morgan, 2000; Stumm and Morgan, 1996). An important aspect of the biogeochemical behaviour of manganese at the Earth's surface is its drastic change in solubility as it changes oxidation state (Burdige, 2006). In oxic environments, under circum-neutral or alkaline pH, manganese is easily oxidised and mainly forms highly insoluble Mn(III/IV) oxides. In acidic and anoxic environments, manganese is present in the reduced and more soluble form, Mn(II) (Post, 1999; Morgan, 2000). In aquatic environments, at fixed temperature and pressure, the biogeochemical behaviour of manganese is controlled by pH, Eh, and the presence of inorganic (e.g., CO_3^{2-}) and organic ligands (Fig. 1.1).

A striking property of manganese oxides in solution is their high capacity to adsorb or incorporate substantial amounts of trace metals (e.g. Cu, Co, Cd, Zn, Ni, Sn, Pb, Ca, Fe, Ra, Hg, U, Pu, Po, As, Se and Th) (Turekian, 1977; Tebo et al. 2004). This “scavenger of the sea” (Goldberg, 1954) affects the distribution of trace metals in the water column and in the sediment to an extent seemingly out of proportion with its concentration (Jenne, 1968; Post, 1999). In sediments, manganese oxides can play an important role as secondary oxidants of organic matter and metabolites (Aller, 1994). When organic matter is remineralised by micro-organisms, the oxidants that provide the greatest amount of free energy in the terminal electron transfer step are utilised first (Froelich *et al.*, 1979; Gaillard *et al.*, 1989). Typically, manganese oxide reduction occurs after oxygen and nitrate have been nearly exhausted and proceeds until nearly all the manganese

oxides is consumed. The soluble Mn(II) produced by this reaction is partitioned between the porewater and the solid sediment phase onto which Mn(II) is known to adsorb (Burdige, 2006). Dissolved Mn(II) can diffuse through the porewater towards the sediment-water interface where it can be oxidized and precipitated as an oxide. It can also diffuse downward into the sediment where it may be precipitated as an authigenic mineral such as a manganoan calcite, rhodochrosite (MnCO_3) or (pseudo)kutnahorite ($\text{Mn}_x\text{Ca}_{1-x}\text{CO}_3$) (Mucci, 2004; Burdige, 2006).

1.3.2 Sediment resuspension

Post-depositional diagenesis is one of the factors that determine metal concentrations, depth distributions and fluxes within the sediment. Another important factor is physical or biological reworking of sediment.

Sediment mixing and particle transport by benthic fauna (bioturbation) can change the geotechnical properties of surface sediments (top 15 cm) (Maurice *et al.*, 2000; Tremblay *et al.*, 2003) and impact the distribution and cycling of redox-sensitive metals such as manganese (Aller, 1990; Burdige, 2006). In environments with a thin oxidised surface layer, benthic organisms displace sediment particles across the oxic-anoxic boundary. Some organisms, living in burrows, excavate and exhume anoxic sediment at the surface. The sharp color contrast between the anoxic (grey) and the oxic (brown) sediment allows this phenomenon to be observed directly in photographs of the seabed (Belley *et al.*, 2010). Upon

exposure to oxygenated bottom water, the anoxic sediment is gradually oxidised and its color changes from grey to brown.

In coastal environments, the most frequent causes of physical disturbance of sediment include: tidal currents, waves, storms, floods, submarine landslides and dredging (e.g. Fanning *et al.*, 1980; Schoellhamer, 1996; Deflandre *et al.*, 2002; Cauchon-Voyer *et al.*, 2008). During such events, the surficial sediment layer is re-suspended, and in some cases, depending on the thickness of this layer and the position of the oxic-anoxic boundary, sediment particles from the anoxic sediment layer can be suspended into the water column.

The exposure of anoxic sediment to oxygenated water reoxidises reduced metal species including manganese. Depending on the rate of Mn(II) oxidation, adsorbed manganese may escape to the water column rather than being immobilised as an insoluble manganese oxide on the sediment particles.

1.3.3 Manganese oxidation kinetics

Laboratory experiments by Morgan and Stumm (1965) and Morgan (1967) first established the autocatalytic character of Mn(II) oxidation. At constant pH and pO₂ and in the absence of a surface, Morgan (1967) showed that the Mn(II) oxidation kinetics is described by the following expression:

$$-\frac{d[Mn(II)]}{dt} = k_1[Mn(II)] + k_2[MnO_x][Mn(II)] \quad (1)$$

where the first and second terms describe, respectively, the homogenous and heterogeneous oxidation paths. In Eqn. (1), k_1 and k_2 are, respectively, first- and

second-order rate constants, and $[\text{MnO}_x]$ denotes the concentration of oxidised manganese species. Homogeneous oxidation of Mn(II) by O_2 is extremely slow (10 million times slower than that of Fe(II) at pH 8 and 25 °C) (Morgan, 2000). The presence of MnO_x and other surfaces such as $\gamma\text{-FeOOH}$, $\alpha\text{-FeOOH}$, SiO_2 and Al_2O_3 surfaces (Sung and Morgan, 1981; Davies and Morgan, 1989) or calcite surfaces (A. Mucci, pers. comm.) catalyzes the rate of Mn(II) oxidation. Manganese oxidation can also be microbially mediated, and many studies have revealed that biological Mn(II) oxidation is faster than abiotic Mn(II) oxidation, including surface-catalyzed reactions (e.g. Hasting and Emerson, 1986; Tebo *et al.*, 1997; Morgan, 2000).

Mn(II) oxidation rates in natural sediments have been determined on slurries of coastal sediment (Edenborn *et al.*, 1985), by combining Mn(II) and O_2 flux measurements with Mn porewater profiles (Thamdrup *et al.*, 1994b) and by fitting Mn porewater profiles to a diagenetic model (Mucci *et al.*, 2003). Unless bacterial poisons are used, the oxidation rates measured in natural sediments include the effects of surface catalysis and microbially-mediated processes.

When anoxic sediments are exposed directly to oxygenated waters, we can assume that the oxidation of Mn(II) is not initially catalyzed by iron and manganese oxide surfaces. This is because, in anoxic sediment, these surfaces are either absent, present in low concentration or, in the case of Fe(III) (hydr)oxide, inactivated by adsorbed and/or surface precipitated Fe(II) (Roden and Urrutia, 1999, 2002). As the reaction proceeds and oxides are precipitated, surface catalysis can become important or dominant. To our knowledge, the oxidation rate

of Mn(II) in anoxic sediment has not yet been measured in the absence of oxidised manganese.

1.3.4 Manganese sorption kinetics

Much attention has been paid to the oxidation kinetics of manganese in sediments, but little is known about its sorption behaviour in anoxic sediments. The few sorption experiments that have been carried out using natural sediments (Taylor, 1987; Canfield *et al.*, 1993) or sedimentary materials (quartz sand, clay, carbonate) (Van der Weijden, 1975) show that: (1) a linear relationship exists between the concentrations of dissolved and adsorbed Mn(II), (2) Mn(II) uptake is proportional to the concentration of particles and (3) the adsorption reaction is rapid (completed within 1 to 3 hours) and irreversible. The rate constants for the Mn(II) adsorption and desorption reactions in anoxic sediment have never been determined experimentally. To our knowledge, the Mn(II) desorption rate constant has been estimated in a single study (Van der Zee *et al.*, 2001), by fitting porewater and solid Mn profiles from continental margin sediments to a reaction-diffusion model.

1.4 Objectives

The objective of this project is to evaluate the plausibility that the advection of anoxic sediment to the sediment-water interface, followed by desorption of dissolved Mn(II) from the particles to the overlying water, may release dissolved manganese from the sediment. To achieve this objective, I determined the relative importance of desorption and oxidation of Mn(II) in natural, anoxic sediments upon their exposure to oxygenated seawater.

1.5 References

- Aller, R. C., 1990. Bioturbation and manganese cycling in hemipelagic sediments. *Philosophical Transactions of the Royal Society A* **331**, 51-68.
- Aller, R. C., 1994. The Sedimentary Mn cycle in Long-Island Sound: its role as intermediate oxidant and the influence of bioturbation, O₂, and C(org) flux on diagenetic reaction balances. *Journal of Marine Research* **52** (2), 259–295.
- Aller, R. C., Aller, J.Y., Kemp, P.F., 2001. Effects of particle and solute transport on rates and extent of remineralization in bioturbated sediments. In: *Organism-Sediment Interactions*. J.Y. Aller, S.A. Woodin, R.C. Aller, (Eds), University of South Carolina Press, Columbia, 315–333.
- Anschutz, P., Sundby, B., Lefrançois, L., Luther III, G.W., Mucci, A., 2000. Interactions between metal oxides and species of nitrogen and iodine in bioturbated marine sediments. *Geochimica et Cosmochimica Acta* **64** (16), 2751–2763.
- Belley, R., Archambault, P., Sundby, B., Gilbert, F., Gagnon, J.-M., 2010. Effects of hypoxia on benthic macrofauna and bioturbation in the Estuary and Gulf of St. Lawrence, Canada. *Continental Shelf Research* **30**, 1302-1313.
- Burdige, D. J., 1993. The biogeochemistry of manganese and iron reduction in marine sediments. *Earth-Science Reviews* **35**, 249–284.
- Burdige, D. J., 2006. *Geochemistry of Marine Sediments*. Princeton University Press. Princeton, 592pp.

- Canfield, D. E., Thamdrup, B., Hansen, J.W., 1993. The anaerobic degradation of organic matter in Danish coastal sediments: Iron, manganese, and sulfate. *Geochimica et Cosmochimica Acta* **57**, 3867-3883.
- Cauchon-Voyer, G., Locat, J., St-Onge, G., 2008. Late-Quaternary morpho-sedimentology and submarine mass movements of the Betsiamites area, Lower St. Lawrence Estuary, Quebec, Canada. *Marine Geology* **251**, 233-252.
- Davies, S.H.R. and Morgan, J.J., 1989. Manganese(II) oxidation kinetics on metal oxide surfaces. *Journal of Colloid and Interface Science* **129**, 63-77.
- Deflandre, B., Mucci, A., Gagné, J-P., Guignard, C., Sundby, S., 2002. Early diagenetic processes in coastal marine sediments disturbed by a catastrophic sedimentation event. *Geochimica et Cosmochimica Acta* **66** (14), 2547-2558.
- Edenborn, H.M., Paquin, Y., Chateauneuf, G., 1985. Bacterial contribution to manganese oxidation in a deep coastal sediment. *Estuarine, Coastal and Shelf Science* **21**, 801-815.
- Fanning, K.A., Carder, K.L., Betzer, P.R., 1980. Sediment resuspension by coastal waters: a potential mechanism for nutrient re-cycling on the ocean's margins. *Deep-Sea Research* **29**, 953-965.
- Froelich, P.N., Klinkhammer, G.P., Bender, M.L., Luedtkeand, N.A., Heath, G.R., Cullen, D., Dauphin, P., Hammond, D., Hartman, B., Maynard, V., 1979. Early oxidation of organic matter in pelagic sediments of the eastern

- equatorial Atlantic: suboxic diagenesis. *Geochimica et Cosmochimica Acta* **43**, 1075–1090.
- Gaillard, J.-F., Pauwels, H., Michard, G., 1989. Chemical diagenesis in coastal marine sediments. *Oceanologica acta* **12**, 175-187.
- Gobeil, C., Macdonald, R.W., Sundby, B., 1997. Diagenetic separation of cadmium and manganese in suboxic continental margin sediments. *Geochimica et Cosmochimica Acta* **61** (21), 4647–4654.
- Goldberg, E.D., 1954. Marine geochemistry I. Chemical scavengers of the sea. *Journal of Geology*. **62**, 249-265.
- Hastings, D. and Emerson, S., 1986. Oxidation of manganese by spores of a marine *Bacillus*: kinetic and thermodynamic considerations. *Geochimica et Cosmochimica Acta* **51**, 1819–24.
- Hem, J.D., 1972. Chemical factors that influence the availability of iron and manganese in aqueous systems. *Geological Society of America Bulletin* **83**, 443-450.
- Jenne, E.A., 1968. Controls on Mn, Fe, Co, Ni, Cu and Zn concentrations in soils and water: the significant role of hydrous Mn and Fe oxides. In: *Trace Inorganics in Water*, Washington, DC. *Journal of the American Chemical Society*, 337–387.
- Kalnejais, L.H., Martin, W.R., Bothner, M.H., 2010. The release of dissolved nutrients and metals from coastal sediments due to resuspension. *Marine Chemistry* **121**, 224-235.
- Maurice, F., Locat, J., and Leroueil, S., 2000. Caractéristiques géotechniques et évolution de la couche de sédiment déposée lors du déluge de 1996 dans la

- Baie des Ha! Ha! (Fjord du Saguenay, Québec). *Proceedings of the 53rd Canadian Geotechnical Conference, Montréal*, 123-130.
- McCaffrey, R.J., Myers, A.C., Davey, E., Morrison, G., Bender, M., Luedtke, N., Cullen, D., Froelich, P., Klinkhammer, G., 1980. The relation between pore water chemistry and benthic fluxes of nutrients and manganese in Narragansett Bay. *Limnology and Oceanography* **25** (1), 31-44.
- Morgan, J.J., 1967. Chemical equilibria and kinetic properties of manganese in natural waters. In: *Principles and Applications in Water Chemistry*, S. Faust and J.V. Hunter, (Eds), John Wiley, New York, 561-622
- Morgan, J.J., 2000. Manganese in natural waters and Earth's crust: Its availability to organisms. In: *Metal Ions in Biological Systems, Manganese and Its Role in Biological Processes*, A. Sigel, H. Sigel, (Eds), New York: Marcel Dekker **37**, 1-33.
- Morgan, J.J. and Stumm, W., 1965. The role of multivalent metal oxides in limnological transformations, As exemplified by iron and manganese. *Proceedings of the Second International Conference on Water Pollution Research*. (Tokyo), Pergamon, Oxford, 103-131.
- Mucci, A., 2004. The behavior of mixed Ca-Mn carbonates in water and seawater: controls of manganese concentrations in marine porewaters. *Aquatic Geochemistry* **10**, 139-169.
- Mucci, A., Boudreau, B., Guignard, C., 2003. Diagenetic mobility of trace elements in sediments covered by a flash flood deposit: Mn, Fe and As. *Applied Geochemistry* **18**, 1011-1026.

- Post, J.E., 1999. Manganese oxide minerals: Crystal structures and economic and environmental significance. *Proceedings of the National Academy of Sciences USA* **96**, 3447-3454.
- Roden E.E. and Urrutia M.M., 1999. Ferrous iron removal promotes microbial reduction of crystalline iron(III) oxides. *Environmental Science & Technology* **33**, 1847–1853.
- Roden E.E. and Urrutia M.M., 2002. Influence of biogenic Fe(II) on bacterial crystalline Fe(III) oxide reduction. *Geomicrobiology Journal* **19**, 209–251.
- Saulnier, I. and Mucci, A., 2000. Trace metal remobilization following the resuspension of estuarine sediments: Saguenay Fjord, Canada. *Applied Geochemistry* **15**, 203–222.
- Schoellhamer, D.H., 1996. Anthropogenic sediment resuspension mechanisms in a shallow microtidal estuary. *Estuarine, Coastal and Shelf Science* **43**, 533-548.
- Schink, D. R. and Guinasso, N. L., 1978. Redistribution of dissolved and adsorbed materials in abyssal marine sediments undergoing biological stirring. *American Journal of Science* **278**, 687-702.
- Stumm, W. and Morgan, J. J., 1996. *Aquatic Chemistry: Chemical Equilibria and Rates in Natural Waters*. John Wiley & Sons, New York.
- Sundby, B., 2006. Transient state diagenesis in continental margin muds. *Marine Chemistry* **102**, 2-12.

- Sundby, B., Silverberg, N., Chesselet, R., 1981. Pathways of manganese in an open estuarine system. *Geochimica et Cosmochimica Acta* **45** (3), 293–307.
- Sung, W. and Morgan, J.J., 1981. Oxidative removal of Mn(II) from solution catalyzed by the γ -FeOOH (lepidocrocite) surface. *Geochimica et Cosmochimica Acta* **45**, 2377-2382.
- Taylor, R. J., 1987. Manganese Geochemistry in Galveston Bay Sediment. Ph.D. dissertation. Texas A&M Univ. 258 pp.
- Taylor, S.R., 1964. Abundance of chemical elements in the continental crust: a new table. *Geochimica et Cosmochimica Acta* **28** (8), 1273–1285.
- Tebo, B.M., Bargar, J.R., Clement, B.G., Dick, G.J., Murray, K.J., Parker, D., Verity, R., Webb, S.M., 2004. Biogenic manganese oxides: properties and mechanisms of formation. *Annual Review of Earth and Planetary Sci.* **32**, 287-328.
- Tebo, B.M., Ghiorse, W.C., van Waasbergen, L.G., Siering, P.L., Caspi, R., 1997. Bacterially mediated mineral formation: insights into manganese(II) oxidation from molecular genetic and biochemical studies. In: *Geomicrobiology: Interactions Between Microbes and Minerals*. JF Banfield, KH Nealson, (Eds), Washington, DC. *Journal of the American Chemical Society*, 225–66.
- Thamdrup, B., Fossing, H., Jørgensen, B.B., 1994a. Manganese, iron, and sulfur cycling in a coastal marine sediment, Aarhus Bay, Denmark. *Geochimica et Cosmochimica Acta* **58** (23), 5115–5129.

- Thamdrup, B., Glud, R.N., Hansen, J.W., 1994b. Manganese oxidation and in-situ manganese fluxes from a coastal sediment. *Geochimica et Cosmochimica Acta* **58** (11), 2563–2570.
- Trefry, J. and Presley, J., 1982. Manganese fluxes from the Mississippi Delta sediments. *Geochimica et Cosmochimica Acta* **46** (10), 1715–1726.
- Tremblay, H., Desrosiers, G., Locat, J., Mucci, A., Pelletier, É., 2003. Characterization of a catastrophic flood sediment layer: geological, geotechnical, biological, and geochemical signatures. In: *Contaminated Sediments: Characterization, Evaluation, Mitigation, Restoration, and Management Strategy Performance*. J. Locat, R. Galvez-Cloutier, R. Chaney, K. Demars, (Eds), ASTM International, West Conshohocken, 87-101.
- Turekian, K.K., 1977. The fate of metals in the ocean. *Geochimica et Cosmochimica Acta* **41** (8), 1139-1144.
- Van der Weijden, C.H., 1975. Sorption Experiments Relevant to the Geochemistry of Manganese Nodules. Ph.D. dissertation. University of Utrecht. 154 pp.
- van der Zee, C., van Raaphorst, W., Epping, E., 2001. Absorbed Mn^{2+} and Mn redox cycling in Iberian continental margin sediments (northeast Atlantic Ocean). *Journal of Marine Research* **59** (1), 133–166.
- Yeats, P. A., Sundby, B., Bowers, J. M., 1979. Manganese recycling in coastal waters. *Marine Chemistry* **8**, 43-55.

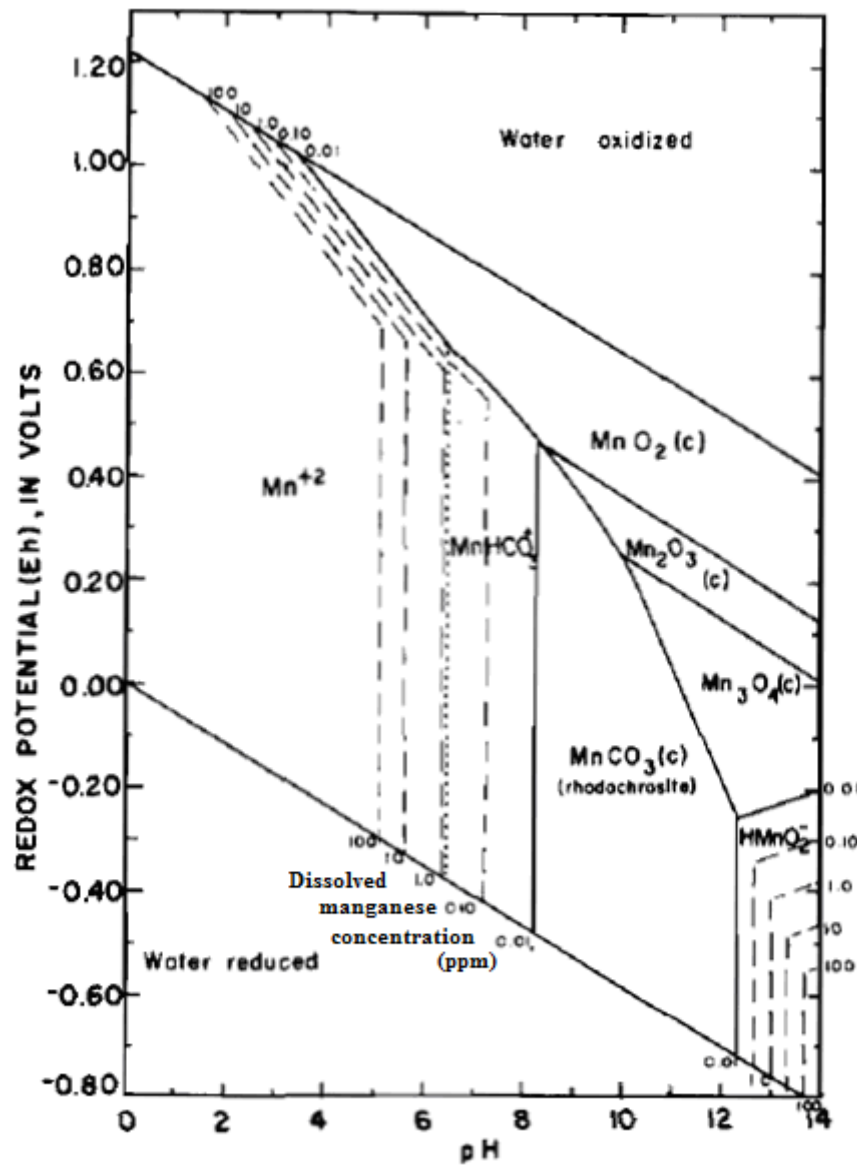


Figure 1.1 – Fields of stability of dissolved species and solids phases of Mn as a function of pH and Eh at 25°C and 1 atm in the Mn-CO₂-H₂O system. Bicarbonate species concentration: 2 mg/L. Modified from Hem (1972).

Chapter 2. Kinetics of manganese adsorption, desorption, and oxidation in coastal marine sediments

2.1 Introduction

In sediments, manganese cycles across the oxic-anoxic boundary via burial of oxidised manganese below the boundary, reductive dissolution, upward diffusion of porewater Mn(II) across the boundary, and its oxidation and re-precipitation in the oxic surface sediment. This cycle enriches the oxic surface sediment in manganese at the expense of the anoxic subsurface sediment. In coastal organic-rich environments, the oxidant demand by the sediment is often high and, consequently, the oxic-anoxic boundary is located near the sediment-water interface. Under these circumstances, dissolved manganese may escape the sediment and be released to the water column. For some coastal environments, mass balance considerations have revealed a net export of manganese from the sediment to the overlying water and out of the system (Sundby *et al.*, 1981; Trefry and Presley, 1982). For example, for Estuary and Gulf of St. Lawrence, Sundby *et al.* (1981) estimated that 5.0×10^9 g/yr of manganese, which is 50% more than the river input of dissolved manganese, escape the sediment and are exported to the open ocean in the suspended matter load.

Mechanisms that can contribute to the dissolved manganese flux out the sediment include: diffusion across the sediment-water interface (McCaffrey *et al.*,

1980; Sundby *et al.*, 1981), porewater advection (McCaffrey *et al.*, 1980), and migration of the Mn(II)/Mn(IV) redox boundary towards the sediment surface (Sundby, 2006). Physical or biological advection of anoxic sediment may also contribute to the dissolved manganese flux (Schink and Guinasso, 1978; Saulnier and Mucci, 2000). As anoxic sediments are resuspended, manganese may be desorbed from sediment particles and released to the water column. This mechanism, which has received little attention, is the subject of this paper.

A variety of different processes such as bioturbation, tidal currents, waves, storms, floods, submarine landslides and dredging can lead to sediment resuspension in coastal environments (e.g. Fanning *et al.*, 1980; Schoellhamer, 1996; Deflandre *et al.*, 2002; Burdige, 2006; Cauchon-Voyer *et al.*, 2008). In sediments with a thin oxidised surface layer, such resuspension events can expose anoxic sediment to the water column, thereby facilitating exchange of soluble sediment constituents with the water column. In the sediment, a fraction of the Mn(II) produced by the reductive dissolution of manganese oxides adsorbs onto sediment particles while the rest remains in the porewater (Van der Zee *et al.*, 2001; Sundby, 2006). The upward diffusing dissolved Mn(II) crosses the redox boundary into the oxic surface layer and in part or completely precipitates as an authigenic oxide. In contrast, resuspended Mn(II)-laden particles completely bypass this trap and adsorbed Mn(II) is exposed directly to the water column. Unlike the anoxic sediment porewater, the overlying water column is typically oxygenated and virtually devoid of dissolved manganese. The sudden exposure of adsorbed Mn(II) to this water triggers two competing reactions: 1) oxidation of

soluble Mn(II) to insoluble Mn(IV), and 2) desorption of Mn(II) to the water column.

Whereas homogeneous oxidation of Mn(II) by O₂ is extremely slow (10 million times slower than oxidation of Fe(II) at pH 8 and 25°C) (Morgan, 2000), in natural sediments, the presence of MnO₂ and other surfaces such as γ -FeOOH, α -FeOOH, SiO₂ and Al₂O₃ surfaces (Sung and Morgan, 1981; Davies and Morgan, 1989) or calcite (A. Mucci, pers. comm.) catalyzes the rate of Mn(II) oxidation. Furthermore, manganese oxidation can also be microbially mediated. Many studies have revealed that biological Mn(II) oxidation is faster than abiotic Mn(II) oxidation, including surface-catalyzed reactions (e.g. Hasting and Emerson, 1986; Tebo *et al.*, 1997; Morgan, 2000).

Much attention has been paid to the oxidation kinetics of manganese in sediments (e.g. Edenborn *et al.*, 1985; Thamdrup *et al.*, 1994a; Mucci *et al.*, 2003), yet, to our knowledge, the oxidation rate of Mn(II) in anoxic sediment has not been measured in the absence of oxidised iron and manganese. Furthermore, little is known about the sorption behavior of manganese in anoxic sediments. The few sorption experiments that have been carried out using natural sediments (Taylor, 1987; Canfield *et al.*, 1993) or sedimentary materials (quartz sand, clay, carbonate) (Van der Weijden, 1975) show that: (1) there is a linear relationship between the concentrations of dissolved and adsorbed Mn(II), (2) Mn(II) uptake is proportional to the concentration of particles and (3) the adsorption reaction is rapid (completed within 1 to 3 hours) and irreversible. The rate constants for Mn(II) adsorption and desorption reactions in anoxic sediment have never been determined experimentally. To our knowledge, the Mn(II) desorption rate

constant has been estimated in a single study (Van der Zee *et al.*, 2001), by fitting porewater and solid phase Mn profiles from continental margin sediments to a reaction-diffusion model.

The amount of Mn(II) released to the overlying water upon advection of anoxic sediment depends on the relative rates of Mn(II) desorption and oxidation at the surface of sediment particles, but the relative rates of these two competing reactions are not known, and it is *a priori* impossible to determine which reaction dominates. In order to evaluate the importance of advection of anoxic sediment on dissolved manganese fluxes to the overlying water column, we measured the rates of adsorption, desorption, and oxidation of Mn(II) by incubating slurries of anoxic sediment recovered from the Lower St. Lawrence Estuary in the presence and absence of oxygen.

2.2 Material and methods

2.2.1 *Environmental setting*

The Lower St. Lawrence Estuary (LSLE) is situated between Tadoussac and Pointes-des-Monts (Fig. 2.1). Its bathymetry is dominated by a more than 300 m deep U-shaped trough, the Laurentian Trough, that extends from the eastern Canadian continental shelf break to Tadoussac. The circulation pattern in the LSLE is estuarine. The bottom water is a mixture of North Atlantic and Labrador Sea water and is unaffected by seasonal variations (Bugden, 1991). The bottom

water in the Lower Estuary has temperatures of 4.5-5.5°C and salinities of 34.2-34.7, and is hypoxic throughout the year with an average O₂ concentration below 62.5 mol/L (Gilbert *et al.*, 2005). The dissolved manganese concentration is <0.5 µmol/L (Yeats *et al.*, 1979).

2.2.2 Sediment characteristics

The sedimentology and lithology of the sediments that cover the Laurentian Through were described by Loring and Nota (1973). The surficial sediment consists of a brown-colored, watery surface layer (<1 cm thick in the LSLE) grading downwards to a homogeneous unstratified olive grey mud containing equal parts of clay and silt-sized particles and 5-10% sand. The mineralogy, dominated by quartz, feldspars, amphiboles, pyroxenes and illite indicates that the sediments are immature. They are principally derived from the mechanical weathering of the crystalline rocks and the Quaternary deposits of the Canadian Shield, and the lithology is nearly invariant with depth into the sediment. The sediments are bioturbated (Silverberg *et al.*, 1986; Belley *et al.*, 2010) and the organic carbon content is ~2% d.w. (Silverberg *et al.*, 1987).

Solid phase manganese is enriched in the surface layer (0-5 mm) of the sediment due to the presence of authigenic manganese oxides (Sundby *et al.*, 1981). Below the sediment-water interface (SWI), the solid phase manganese concentration decreases rapidly as manganese oxides are reductively dissolved and Mn(II) is released to the porewater. Porewater and solid phase (reactive) manganese profiles at Station 23 in the LSLE were obtained by Anschutz *et al.*

(2000). In their solid phase profile (Fig. 2.2A), the reactive manganese concentration reached 93 $\mu\text{mol/g}$ in the surface layer (0-5 mm), and 5 to 10 $\mu\text{mol/g}$ 4 cm below the SWI. Porewater manganese concentrations were first detected (detection limit 5 $\mu\text{mol/L}$) at a depth of 1.3 cm, reached a maximum value of 225 $\mu\text{mol/L}$ 4 cm below the SWI and decreased with depth (Fig. 2.2B).

2.2.3 Sampling and storage

Sediment and bottom water were collected onboard the R/V Coriolis II in July 2009 and 2010 at Station 23 in the Lower St. Lawrence Estuary. Station 23, located in front of Rimouski, has an approximate water depth of 350 m (Fig. 2.1). Undisturbed sediment cores were recovered with an Ocean Instrument Mark II box corer (0.12 m^2). The ~10-30 cm sub-bottom interval, chosen in order to recover anoxic sediment below the manganese reduction zone, was sub-sampled onboard. The sediment was transferred to large Mason jars that were sealed with a layer of Parafilm before being capped and stored at 4°C until the laboratory experiments began. In the laboratory, the Mason jars were brought inside a Coy Lab vinyl anaerobic chamber and opened under a $\text{N}_2\text{-H}_2$ atmosphere. Inside the chamber, the anoxic sediment was homogenised by mixing in a ceramic bowl with a plastic spatula at room temperature. The homogenised sediment was then transferred to a large beaker, sealed with Parafilm, and kept in the anaerobic chamber at room temperature until needed for analysis and slurry incubation experiments.

Bottom water was collected at ~335 m depth using 12-L PVC Niskin bottles mounted on a CTD/rosette. The salinity of the water was 34.52, as determined by the calibrated conductivity probe of the CTD (SeaBird SBE 911). The seawater was brought back to the laboratory in 25-L polyethylene containers previously washed with Milli-Q water. In the laboratory, approximately 10 L of the seawater were filtered through a 0.45 μm Millipore polycarbonate filter. The filtered seawater was stored at room temperature in a clean screw-cap polypropylene container until needed for the slurry experiments. The dissolved Mn concentration of the seawater was $< 1 \mu\text{mol/L}$ (see section 2.2.6 for analytical procedure).

2.2.4 Sediment and porewater analyses

A pre-weighed aliquot of homogenised sediment was freeze-dried and re-weighed to determine the water content. The reproducibility of the measurement was better than 0.1% (see Table 2.1). The freeze-dried sediment, homogenised by grinding with an agate mortar and pestle, was used to determine the reactive Mn content according to the method described by Leventhal and Taylor (1990) and Raiswell *et al.* (1994). Briefly, reactive manganese was extracted for 24 h with a 1 N HCl solution at a solid:solution ratio of 1:50. Prior to analysis, the extracts were filtered through a 0.45 μm Millipore polycarbonate filter and diluted with Milli-Q water. Before each slurry incubation experiment, porewater was extracted by centrifuging a few grams of the homogenised wet sediment. To prevent oxidation artefacts, the centrifuge tubes were filled in the anaerobic chamber and returned to

the anaerobic chamber after centrifugation. The porewater was immediately syringe filtered through a 0.45 μm Millipore polycarbonate filter and acidified with a 1% equivalent volume of concentrated HCl before being stored at 4°C for later Mn analysis. The measured porewater Mn concentrations were used to calculate the initial dissolved manganese concentration in the slurry experiments.

Dissolved Mn concentrations (porewater and extracts) were determined by atomic absorption spectrometry (AAS; Perkin-Elmer AAnalyst-100) with an air-acetylene flame and an impact bead burner. External aqueous AAS standards were prepared by appropriate dilution of a 1000 ppm certified solution (Plasmacal, ICP-AES and ICP-MS standard, NIST-traceable prepared in 4% HNO_3) in a NaCl solution of ionic strength corresponding to the samples and acidified with a 1% equivalent volume of concentrated HCl. The reproducibility of the measurements was better than 5% and the detection limit was $<1 \mu\text{M}$.

2.2.5 Slurry incubation experiments

The adsorption, desorption and oxidation rates of manganese in natural sediment were determined by monitoring the evolution of dissolved manganese over time in dilute sediment suspensions at 25°C. Slurry incubation experiments were conducted in duplicate in separate reactors and were designed to individually measure the kinetics of Mn(II) adsorption, desorption and oxidation. First, adsorption or desorption was initiated by mixing wet anoxic sediment and seawater under anaerobic conditions. Second, once the adsorption or desorption

experiments reached steady state, the oxidation reaction was initiated by exposing the slurry to oxygen. Throughout the experiments, aliquots of the slurries were taken at fixed time intervals, filtered and analysed for dissolved Mn, as described above (section 2.2.4). The aliquots were assumed to have the same solid:solution ratio as the slurries and were not replaced in the reaction vessels as the experiments progressed. The solid:solution ratio for the experiments was such that it provided enough solution to perform the analyses. The initial conditions for the slurry incubation experiments are presented in Table 2.2.

2.2.5.1 Adsorption and desorption experiments

The desorption experiments were initiated by resuspending a set amount (Table 2.2) of homogenised wet sediment in filtered LSLE bottom seawater containing less than 0.5 $\mu\text{mol/L}$ Mn. The adsorption experiments were carried out in a similar manner except that the sediment was resuspended in filtered LSLE seawater to which MnCl_2 was added to obtain dissolved Mn concentrations between 115 and 130 $\mu\text{mol/L}$. The particles were maintained in suspension during the experiments by mounting the 400 mL water-jacketed glass reactors on a VWR Scientific orbital shaker set at 160 RPM. The reactors were closed by rubber stoppers with holes for the pH electrode and gas delivery tubes and the temperature was maintained constant by circulating water from a constant temperature bath (at 25°C) through the exterior glass jacket. A schematic diagram of the reactor is presented in Figure 2.3. The adsorption/desorption experiments were conducted in a glove bag continuously purged with a stream of a

commercially-prepared CO₂-N₂ gas mixture (pO₂<1 ppmv, pCO₂ = 1000 ppmv). This gas mixture also flowed through the reaction vessels. The partial pressure of the CO₂ in the gas mixture was chosen to best reproduce the *in-situ* pCO₂ and pH conditions of LSLE bottom water (pCO₂ ≈ 1000 ppmv; pH_{sws} = 7.69 at 25°C).

Prior to conducting the adsorption and desorption experiments, 300 mL of filtered LSLE bottom seawater were placed in each reaction vessel and purged overnight with the N₂-CO₂ gas mixture. A few mL of the seawater were transferred to acid-cleaned plastic bottles for later analysis of the initial dissolved manganese concentration. The initial dissolved Mn concentration in the slurries (at time = 0) was calculated by assuming that the seawater and porewater Mn mixed conservatively. The adsorption/desorption experiments were initiated by mixing a few grams (~18 or ~30) of wet, anoxic sediment with the seawater in the reactors. The homogenised wet sediment used for the experiments had previously been transferred inside the glove bag after being quickly weighed out. Most of the adsorption/desorption experiments were conducted at a solid:solution ratio of ~ 43 g/L. One desorption experiment was conducted at a solid:solution ratio of 26 g/L (see Table 2.2). During the first minute of the experiments, the slurries were stirred manually with a plastic spatula to break up wet sediment clumps. The reactors were then capped and mounted on the orbital shaker. At different time intervals over a period of 7 to 95 h, 8 to 10 5-mL aliquots of the slurry were sampled. The aliquots were collected with a pipette and immediately filtered through a 0.45 µm Millipore polycarbonate filter. Filtered samples were taken out of the glove bag and transferred to acid-cleaned plastic bottles, acidified with a

1% equivalent volume of concentrated HCl, and stored at 4°C until analysis (see section 2.2.4).

2.2.5.2 *Oxidation experiments*

The oxidation experiments were initiated by purging the reactors with ambient air after the completion of the adsorption/desorption experiments. Over the next 45 to 179 h, 8 to 10 5-ml aliquots of the slurries were sampled at different time intervals. Each aliquot was immediately filtered through a 0.45 μm Millipore polycarbonate filter, acidified with a 1% equivalent volume of concentrated HCl, and stored at 4°C until analysis (see section 2.2.4).

2.2.5.3 *pH measurements*

pH measurements on the seawater scale (pH_{sws}) were carried out at regular intervals throughout the slurry incubation experiments using a combination glass-reference electrode (model 6.0259.100 Unitrode; Metrohm) and pH-meter (model 713; Metrohm). The orbital shaker was stopped during the pH measurements. Before and after each measurement, the electrode was calibrated using three NIST-traceable buffer solutions (4.01, 7.00, 10.00 at 25°C) and a TRIS (Tris(hydroxymethyl)aminomethane) seawater buffer solution of salinity 33.55 (Millero *et al.*, 1993). The Nernstian response of the electrode was obtained from the three NIST-traceable buffers and corrected to the seawater scale using the TRIS buffer.

2.2.5.4 HEPES buffer

In an attempt to minimize pH variations observed during the oxidation experiments, HEPES buffer (N-2-hydroxyethylpiperazine-N'-2-ethanesulfonic acid) was added to the seawater before the sediment was resuspended (Exp. # 10-11, #12-13). The HEPES buffer does not interfere with Mn(II) sorption onto δMnO_2 nor does it solubilise this mineral (Rosson *et al.*, 1984). The buffer concentrations used are given in table 2.2.

2.3 Results and discussion

2.3.1 Desorption and adsorption experiments

During each of the three desorption experiments, the dissolved manganese concentration initially rose rapidly, settled back down over the next few hours, before reaching a constant value for the remainder of the experiment (Fig. 2.4A, Table 2.3). Presumably, the constant concentration represents a steady state between desorption and adsorption. At the higher solid:solution ratio (43 g/L; Exp. #4-5 and #10-11), the steady state concentration was 10-15 $\mu\text{mol/L}$. It was slightly lower, 5.7-8.6 $\mu\text{mol/L}$, at the lower solid:solution ratio (26 g/L, Exp. #8-9). The ratio of the steady-state dissolved manganese concentration to the mass of solid sediment (dry weight) was nearly identical in the three experiments ($0.30 \pm 0.05 \mu\text{mol/g dw}$) (Fig 2.4B). These results suggest that manganese desorption

from natural LSLE sediment cannot be represented by a reversible adsorption-desorption equilibrium, but that a fixed amount of manganese is released to solution per unit mass of anoxic sediment exposed to manganese-free seawater. In other words, the steady state can be represented by:

$$[\text{Mn}_{\text{diss}}]/[\text{solid}] = \text{constant} \quad (1)$$

Within the narrow range investigated (115-130 $\mu\text{mol/L}$), the dissolved manganese concentration decreased rapidly in both sets of adsorption experiments (Exp. #6-7 and #12-13), reaching a steady state at 58-70 $\mu\text{mol/L}$ within the first hour (Fig. 2.5A, Table 2.4). Like the desorption experiments, the dissolved manganese concentrations evolved beyond the steady state value before settling to a time-invariant value. Given the initial (115-130 $\mu\text{mol/L}$) and steady state (65 $\mu\text{mol/L}$) dissolved manganese concentrations and the experimental solid:solution ratio, we estimated that 1.45 to 1.70 $\mu\text{mol Mn/g dw}$ was adsorbed. This estimate agrees reasonably well with the results of similar experiments conducted by Canfield *et al.* (1993) who reported that between 1.25 and 1.5 $\mu\text{mol Mn/g dw}$ adsorbed onto anoxic sediments from the Skagerrak when exposed to solutions containing 100 and 150 $\mu\text{mol/L}$ of manganese.

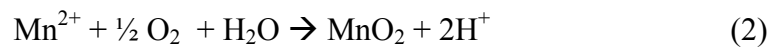
The steady state values measured in adsorption experiments carried out with and without the HEPES buffer (respectively Exp. #12-13 and #6-7) are identical within one standard deviation of their respective means. The steady state values measured in desorption experiments carried out with and without the HEPES buffer (respectively Exp. #10-11 and #4-5) are identical within two standard deviations of their respective means. In the presence or absence of the

HEPES buffer, pH_{SWS} remained stable at 7.7 ± 0.05 throughout the desorption (Table 2.3) and adsorption (Table 2.4) experiments.

2.3.2 Oxidation experiments

A total of four oxidation experiments were conducted. Two followed desorption experiments (Exp. #4-5 and #10-11) and two followed adsorption experiments (Exp. #6-7 and #12-13), and all four were conducted at different initial dissolved manganese concentrations. In all cases, the dissolved manganese concentrations decreased over the course of 50 to 150 hours until they became undetectable (Fig. 2.6A, Table 2.5).

Unlike the adsorption/desorption experiments, the pH_{SWS} varied significantly during the oxidation experiments (Fig. 2.6B Table 2.5). During the first few hours of the oxidation experiments, the pH_{SWS} rose rapidly before decreasing gradually until the end of the experiment. The observed pH increase is caused by the decrease in pCO₂ (from 1000 ppmv to 380 ppmv) as the reactors were purged with ambient air instead of the N₂-CO₂ gas mixture. The decrease in pH that follows is explained by the mass action equation describing the Mn(II) oxidation:



The largest pH_{SWS} variations were observed in the two experiments carried out in the absence of the HEPES buffer (Exp. # 4-5 and # 6-7). In these experiments, pH varied by 0.43 and 0.50 respectively. In the other two experiments (Exp. #10-11 and #12-13), two different concentrations of the HEPES buffer were added in

order to minimize pH_{SWs} variations. In the presence of 5 mM HEPES buffer (Exp. # 10-11), pH_{SWs} varied by 0.21, whereas at 20 mM HEPES (Exp. #12-13) it varied only by 0.17. The presence of HEPES buffer did not interfere with the manganese oxidation.

2.3.3 Adsorption and desorption kinetics

In both the adsorption and the desorption experiments, the dissolved manganese concentrations changed rapidly at the beginning of the experiments before reaching a steady state (Fig. 2.4A and 2.5A). The data obtained during this early stage of the reactions can be used to derive kinetic rate constants. To describe the rates of the adsorption and desorption reactions, we assume that both reactions can be represented by first-order kinetics. The first-order rate law for the desorption (3a) and adsorption (3b) reactions are:

$$\frac{d}{dt} [\text{Mn}_{\text{diss}}] = k_{\text{des}}' [\text{Mn}_{\text{ads}}] = k_{\text{des}}' ([\text{Mn}_{\text{ss}}] - [\text{Mn}_{\text{diss}}]) \quad (3a)$$

and

$$\frac{d}{dt} [\text{Mn}_{\text{diss}}] = k_{\text{ads}}' ([\text{Mn}_{\text{diss}}] - [\text{Mn}_{\text{ss}}]) \quad (3b)$$

where $[\text{Mn}_{\text{ads}}]$, $[\text{Mn}_{\text{ss}}]$ and $[\text{Mn}_{\text{diss}}]$ are the adsorbed, steady-state and dissolved concentrations of manganese and k' is the first-order reaction rate constant. In terms of modeling, the adsorption and desorption reactions can also be represented by the following first-order rate equation:

$$\frac{d}{dt} [\text{Mn}_{\text{diss}}] = k' [\text{Mn}_{\text{diss}}] \quad (4)$$

The integrated solution of Eq. (4) is:

$$\ln \frac{[\text{Mn}_{\text{diss}}]_t}{[\text{Mn}_{\text{diss}}]_0} = k't \quad (5)$$

where the subscripts 0 and t denote time zero and time t , respectively. If the reaction rate can be described by first-order kinetics, a plot of $\ln ([\text{Mn}_{\text{diss}}]_t/[\text{Mn}_{\text{diss}}]_0)$ versus time will give a straight line with a slope of k' (k_{des}' or k_{ads}' for the desorption and adsorption reactions, respectively).

First-order kinetics plots, based on the time evolution of dissolved manganese concentrations in our adsorption and desorption experiments, are presented in Figure 2.7 and 2.8. The first few minutes of the reactions are well described by a first-order rate law with first-order rate constants (k_{des}') of $0.21 \pm 0.06 \text{ min}^{-1}$ ($r^2 = 0.48$ – Fig. 2.7) and (k_{ads}') of $0.12 \pm 0.06 \text{ min}^{-1}$ ($r^2 = 0.52$ – Fig. 2.8). The uncertainty of the slopes (k_{des}' or k_{ads}') corresponds to the 95% confidence interval of the least squares regressions.

This is the first time that manganese adsorption and desorption rates on natural anoxic sediments have been measured directly. Van der Zee *et al.* (2001) estimated a first-order rate constant for manganese desorption in anoxic sediments from the Iberian continental margin by fitting porewater and solid Mn profiles to a reaction-diffusion model. Their estimated first-order desorption rate constant (0.0004 to 0.6 d^{-1}) is 3.5 to 6 orders of magnitude smaller than our value (0.21 min^{-1} or 305 d^{-1}).

2.3.4 Oxidation kinetics

Manganese concentrations decreased over time throughout our oxidation experiments (Figure 2.6A). Given the autocatalytic nature of the Mn(II) oxidation reaction (Morgan and Stumm, 1965), we can assume that, as MnO₂ started precipitating, it adsorbed Mn(II) and catalyzed the reaction. Other factors that may have influenced the oxidation rate, given the complexity of our experimental natural substrate and since bacterial poisons were not used in our experiments, include bacterial-mediation (Tebo *et al.*, 2004) and surface catalysis by iron oxides or other particles (Davies and Morgan, 1989). Whereas adsorption and desorption reactions take place within minutes (see section 2.3.3.1), our data show that oxidation proceeds over many hours (Figure 2.6A). In order to derive a rate constant for the homogeneous (i.e. non-catalyzed) oxidation reaction, with the purpose of comparing it to the adsorption and desorption rates on similar time scales, we focused only on the first few hours of the oxidation experiments. In other words, we assumed that, at the beginning of the experiments, when the availability of MnO₂ surfaces is limited, the reaction is not auto-catalyzed and can be represented by pseudo-first-order kinetics (Eq. 4) where k_{ox}' is the first-order oxidation reaction rate constant. A first-order kinetics plot showing the temporal evolution of dissolved manganese in our combined oxidation experiments is presented in Figure 2.9 (see Eq.5 and description below). The first few hours of the oxidation reaction are well described by a first-order rate law with a first-order rate constant (k_{ox}') of $0.020 \pm 0.006 \text{ h}^{-1}$ ($r^2 = 0.52$ – Fig. 2.9). The uncertainty of the slope (k_{ox}') represents a 95% confidence interval of the least squares regression.

As the experiments progress past the first 12 to 20 hours, deviations from the log-linear fit suggest that the oxidation reaction has become auto-catalyzed (Stumm and Morgan, 1996).

When comparing the value obtained in the present study to values reported in the literature (Table 2.6), it is important to keep in mind that our rate constant describes only the first few hours of the reaction. The first-order oxidation rate constant we measured is smaller than all other first-order rate constants reported for coastal sediments because the latter include a component of the surface-catalyzed reactions and, in some cases, a component of microbial oxidation. Edenborn *et al.* (1985) derived Mn(II) first-order oxidation rate constants by conducting slurry experiments with surface sediments from the LSLE. Their values decreased by more than two orders of magnitude with sediment depth over the first 30-mm interval, as the availability of MnO₂ and FeO_x reactive sites decreased with depth (see Fig. 2.2A). The first-order oxidation rate constant we measured, 0.02 h⁻¹ (96 y⁻¹), is a little more than one order of magnitude smaller than the value (2.4 x 10³ yr⁻¹) they obtained with sediment taken from a depth of 30 mm. A possible explanation for the discrepancy is that our reducing sediment (taken in the 10-30 cm interval) provided even fewer reactive surface sites for catalytic oxidation. For example, Anschutz *et al.* (2000) measured reactive Fe concentrations of ~130 μmol/g dw at 3 cm and <100 μmol/g dw below 10 cm in sediment taken at station 23 in the LSLE (Fig. 2.2A).

2.3.5 Desorption kinetics vs. oxidation kinetics

The first-order desorption and oxidation rate constants we obtained, $k_{des}' = 0.21 \pm 0.06 \text{ min}^{-1}$ ($12.7 \pm 3.3 \text{ h}^{-1}$) and $k_{ox}' = 0.020 \pm 0.006 \text{ h}^{-1}$, indicate that desorption is faster than oxidation under our experimental conditions (25°C, 1 atm., pH_{SWS} = 7.65 to 8). In natural environments, when anoxic sediment is exposed to oxygenated bottom seawater, desorption and oxidation reactions occur simultaneously. A simulation showing the hypothetical temporal evolution of dissolved manganese concentrations as the two reactions occur simultaneously is shown in Figure 2.10. The overall rate of the concurrent reactions is obtained by subtracting the first-order oxidation rate (Eq. 3) from the first-order desorption rate (Eq. 4):

$$R = \frac{d}{dt} [\text{Mn}_{\text{diss}}] = k_{des}' ([\text{Mn}_{\text{diss}}]_{\text{ss}} - [\text{Mn}_{\text{diss}}]) - k_{ox}' [\text{Mn}_{\text{diss}}] \quad (6)$$

The concentration of dissolved manganese as a function of time ($[\text{Mn}_{\text{diss}}]_t$) is calculated using the integrated solution of Eq. (6) :

$$[\text{Mn}_{\text{diss}}]_t = ([\text{Mn}_{\text{diss}}]_{\text{ss}} (1 - e^{-k_{des}'t})) - e^{-k_{ox}'t} \quad (7)$$

In Eq. (7), subscript t denotes time t , and k_{des} and k_{ox} are the first-order desorption and oxidation rate constants obtained under our experimental conditions. The steady state manganese concentration ($[\text{Mn}_{\text{diss}}]_{\text{ss}}$) in this simulation is 12.5 $\mu\text{mol/L}$, corresponding to the mean steady state value for desorption experiments #4-5 and #10-11 at a solid:solution ratio of 43 g/L. According to this simulation, a maximum dissolved manganese concentration of 12.3 $\mu\text{mol/L}$ would be reached within the first 30 minutes of exposing anoxic sediment to oxygenated bottom seawater at a solid/solution ratio of 43 g/L. After reaching a maximum, dissolved

manganese concentrations would decrease over several hours as manganese oxidation and precipitation proceed. The time evolution of dissolved manganese concentrations obtained in this simulation agrees reasonably well with results of an experiment carried out by Saulnier and Mucci (2000) who resuspended anoxic sediment (13-15 cm interval) from the Saguenay Fjord in oxygenated seawater at a solid/solution ratio of 35 g/L. In their experiment, a maximum dissolved manganese concentration of 11.8 $\mu\text{mol/L}$ was reached within the first hour, after which the manganese concentration decreased over the course of many hours. In the experiment by Saulnier and Mucci (2000), dissolved manganese concentrations seem to decrease a little faster than in our simulation. This could be due to scatter in their data or to the fact that our simulation does not include auto-catalytic oxidation kinetics.

In natural aquatic environments, in contrast to closed system experiments (e.g. this study, Saulnier and Mucci, 2000), dissolved manganese would be released to the bottom water and rapidly carried away from the sediment-water interface, thus, preventing re-oxidation at the sediment surface and retention of manganese by the sediment. Hence, in addition to the rapid desorption kinetics and slow oxidation kinetics, the transport of soluble manganese by bottom water would contribute to the overall mechanism by which manganese is released from the sediment following the advection of anoxic sediment to the sediment surface.

In this study, desorption and oxidation rate constants were calculated using data ($[\text{Mn}_{\text{diss}}]$) obtained during the early stages of the reactions, i.e., during the first 15 minutes of desorption and the first 12 hours of oxidation. During these time intervals, the pH_{SWS} in our desorption experiments (7.69 ± 0.04) was

identical to the LSLE bottom water *in-situ* pH ($\text{pH}_{\text{SWS}} = 7.69$ at 25°C), but the pH_{SWS} in our oxidation experiments (7.9 ± 0.1) was slightly higher. pH has been shown to have a strong influence on Mn(II) oxidation rates (Davies and Morgan, 1989; Morgan, 2000): as pH increases, the homogeneous pseudo first-order rate constant for Mn(II) oxidation increases ($k_{\text{ox}}' = k_I[\text{O}_2][\text{OH}^-]^2$) (Morgan, 2000). Therefore, we can assume that the first-order oxidation rate constant we obtained, $k_{\text{ox}}' = 0.020 \pm 0.006 \text{ h}^{-1}$, is an upper limit of the oxidation rate constant at *in-situ* pH_{SWS} conditions (7.69), 25°C , and 1 atmosphere total pressure.

2.3.6 *Caveat*

The data from our adsorption, desorption and oxidation experiments show a significant amount of scatter, probably due, to some extent, to the heterogeneous nature of the sediment. When experimenting with natural sediments of complex mineralogical and chemical composition, the solute of interest (i.e., Mn(II)) may participate in a web of abiotic and microbially-mediated reactions (sorption, precipitation/dissolution, redox) for which the experimentalist may have limited control. Furthermore, because the experiments were carried out with St. Lawrence Estuary sediments, our results may not apply directly to other sedimentary environments. Nevertheless, our interpretations of the relative reaction rates upon exposure of reducing sediments to oxygenated overlying waters are probably valid in most coastal marine environments.

There are significant differences between our experimental conditions and the in-situ environmental conditions they simulate. During our experiments, the slurries are confined within the reaction vessel and resuspension is induced by rotary shaking. These conditions contrast with the unconfined situation at the sediment-water interface and with natural resuspension processes. Other parameters that differ include temperature, pressure, and, in some experiments, pH and pO_2 .

The first-order rate constant we obtained for the oxidation of Mn(II) in anoxic sediment was calculated by measuring the temporal evolution of porewater Mn(II) concentrations during the first 12 hours of our oxidation experiment. It describes the net disappearance rate of dissolved Mn(II) from our experimental slurries including the adsorption and oxidation of porewater Mn(II), but we cannot derive a specific rate constant for the oxidation of adsorbed Mn(II).

2.4 Summary

Using the results we obtained during our slurry incubation experiments, we were able, for the first time, to derive first-order rate constants for the adsorption, desorption and oxidation of dissolved manganese in anoxic sediments. The first-order rate constants we obtained for the adsorption (k_{ads}) and desorption (k_{des}) reactions are $0.12 \pm 0.06 \text{ min}^{-1}$ ($7.0 \pm 3.4 \text{ h}^{-1}$) and $0.21 \pm 0.06 \text{ min}^{-1}$ ($12.7 \pm 3.3 \text{ h}^{-1}$) respectively. Both of these rates are more than two orders of magnitude larger than the first-order oxidation rate constant (k_{ox}) of $0.020 \pm 0.006 \text{ h}^{-1}$ we obtained.

The first-order rate constants for Mn(II) desorption and oxidation indicate that upon exposure of natural anoxic sediment to oxygenated seawater, desorption occurs more rapidly than oxidation. Hence, the advection of reducing sediment by physical or biological processes releases manganese to the water column and contributes to the overall dissolved manganese flux.

References

- Anschutz, P., Sundby, B., Lefrançois, L., Luther III, G.W., Mucci, A., 2000. Interactions between metal oxides and species of nitrogen and iodine in bioturbated marine sediments. *Geochimica et Cosmochimica Acta* **64** (16), 2751–2763.
- Belley, R., Archambault, P., Sundby, B., Gilbert, F., Gagnon, J.-M., 2010. Effects of hypoxia on benthic macrofauna and bioturbation in the Estuary and Gulf of St. Lawrence, Canada. *Continental Shelf Research* **30**, 1302–1313.
- Bugden, G.L., 1991. Changes in the temperature–salinity characteristics of the deeper waters of the Gulf of St. Lawrence over the past several decades. In: *The Gulf of St. Lawrence: Small Ocean or Big Estuary?* Therriault, J.-C. (Ed), *Canadian Special Publication of Fisheries and Aquatic Sciences* **113**, 139–147.
- Burdige, D. J., 2006. *Geochemistry of Marine Sediments*. Princeton University Press. Princeton, 592pp.
- Canfield, D. E., Thamdrup, B., Hansen, J.W., 1993. The anaerobic degradation of organic matter in Danish coastal sediments: iron, manganese, and sulfate. *Geochimica et Cosmochimica Acta* **57**, 3867–3883.
- Cauchon-Voyer, G., Locat, J., St-Onge, G., 2008. Late-Quaternary morpho-sedimentology and submarine mass movements of the Betsiamites area, Lower St. Lawrence Estuary, Quebec, Canada. *Marine Geology* **251**, 233–252.

- Davies, S.H.R. and Morgan, J.J., 1989. Manganese(II) oxidation kinetics on metal oxide surfaces. *Journal of Colloid and Interface Science* **129**, 63-77.
- Dhakar, S.P., Burdige, D.J., 1996. A coupled, non-linear, steady state model for early diagenetic processes in pelagic sediments. *American Journal of Science* **296**, 296–330.
- Deflandre, B., Mucci, A., Gagné, J-P., Guignard, C., Sundby, S., 2002. Early diagenetic processes in coastal marine sediments disturbed by a catastrophic sedimentation event. *Geochimica et Cosmochimica Acta* **66** (14), 2547-2558.
- Edenborn, H.M., Paquin, Y., Chateaufneuf, G., 1985. Bacterial contribution to manganese oxidation in a deep coastal sediment. *Estuarine, Coastal and Shelf Science* **21**, 801-815.
- Fanning, K.A., Carder, K.L., Betzer, P.R., 1980. Sediment resuspension by coastal waters: a potential mechanism for nutrient re-cycling on the ocean's margins. *Deep-Sea Research* **29**, 953-965.
- Gilbert, D., Sundby, B., Gobeil, C., Mucci, A., Tremblay, G.H., 2005. A seventy-year record of diminishing deep-water oxygen levels in the St. Lawrence Estuary—the northwest Atlantic connection. *Limnology and Oceanography* **50**, 1654– 1666.
- Gratton, Y., Edenborn, H.M., Silverberg, N., Sundby, B., 1990. A mathematical model for manganese diagenesis in bioturbated sediments. *American Journal of Science* **290**, 246–262.

- Hastings, D. and Emerson, S., 1986. Oxidation of manganese by spores of a marine *Bacillus*: kinetic and thermodynamic considerations. *Geochimica et Cosmochimica Acta* **51**, 1819–24.
- Leventhal, J. and Taylor, C., 1990. Comparison of methods to determine degree of pyritization. *Geochimica et Cosmochimica Acta* **54**, 2621–2625.
- Loring, D.H. and Nota, D.J., 1973. Morphology and sediments of the Gulf of St. Lawrence. *Bulletin of the Fisheries Research Board of Canada* **182**, 147.
- McCaffrey, R.J., Myers, A.C., Davey, E., Morrison, G., Bender, M., Luedtke, N., Cullen, D., Froelich, P., Klinkhammer, G., 1980. The relation between pore water chemistry and benthic fluxes of nutrients and manganese in Narragansett Bay. *Limnology and Oceanography* **25** (1), 31-44.
- Millero F. J., Zhang J.-Z., Fiol S., Sotolongo S., Roy R. N., Lee K., Mane S., 1993. The use of buffers to measure the pH of seawater. *Marine Chemistry* **44**, 143–152.
- Morgan, J.J., 2000. Manganese in natural waters and Earth's crust: Its availability to organisms. In: *Metal Ions in Biological Systems, Manganese and Its Role in Biological Processes*, A. Sigel, H. Sigel (Eds.), New York: Marcel Dekker **37**, 1–33.
- Morgan, J.J. and Stumm, W., 1965. The role of multivalent metal oxides in limnological transformations, as exemplified by iron and manganese. *Proceedings of the Second International Conference on Water Pollution Research*. (Tokyo), Pergamon, Oxford, pp. 103-131.

- Mucci, A., Boudreau, B., Guignard, C., 2003. Diagenetic mobility of trace elements in sediments covered by a flash flood deposit: Mn, Fe and As. *Applied Geochemistry* **18**, 1011-1026.
- Raiswell, R., Canfield, D.E., Berner, R.A., 1994. A comparison of iron extraction methods for the determination of degree of pyritisation and the recognition of iron-limited pyrite formation. *Chemical Geology* **111**, 101–110.
- Rosson, R.A., Tebo, B.M., Nealson, K.H., 1984. Use of poisons in determination of microbial manganese binding rates in seawater. *Applied and Environmental Microbiology*, 740-745.
- Saulnier, I. and Mucci, A., 2000. Trace metal remobilization following the resuspension of estuarine sediments: Saguenay Fjord, Canada. *Applied Geochemistry* **15**, 203–222.
- Schink, D. R. and Guinasso, N. L., 1978. Redistribution of dissolved and adsorbed materials in abyssal marine sediments undergoing biological stirring. *American Journal of Science* **278**, 687-702.
- Schoellhamer, D.H., 1996. Anthropogenic sediment resuspension mechanisms in a shallow microtidal estuary. *Estuarine, Coastal and Shelf Science* **43**, 533-548.
- Silverberg, N., Bakker, J., Edenborn, H.M., Sundby, B., 1987. Oxygen profiles and organic carbon fluxes in Laurentian Trough sediments. *Netherlands Journal of Sea Research* **21**, 95– 105.
- Silverberg N., Nguyen H. V., Delibrias G., Koide M., Sundby B., Yokoyama Y., Chesselet R., 1986. Radionuclide profiles, sedimentation rates, and

- bioturbation in modern sediments of the Laurentian Trough, Gulf of St. Lawrence. *Oceanologica Acta* **9**, 285–290.
- Stumm, W. and Morgan, J. J., 1996. *Aquatic Chemistry: Chemical Equilibria and Rates in Natural Waters*. John Wiley & Sons, New York, 1003 pp.
- Sundby, B., 2006. Transient state diagenesis in continental margin muds. *Marine Chemistry* **102**, 2–12.
- Sundby, B., Silverberg, N., Chesselet, R., 1981. Pathways of manganese in an open estuarine system. *Geochimica et Cosmochimica Acta* **45** (3), 293–307.
- Sung, W. and Morgan, J.J., 1981. Oxidative removal of Mn(II) from solution catalyzed by the γ -FeOOH (lepidocrocite) surface. *Geochimica et Cosmochimica Acta* **45**, 2377–2382.
- Taylor, R. J., 1987. Manganese Geochemistry in Galveston Bay Sediment. Ph.D. dissertation. Texas A&M Univ. 258 pp.
- Thamdrup, B., Fossing, H., Jørgensen, B.B., 1994a. Manganese, iron, and sulfur cycling in a coastal marine sediment, Aarhus Bay, Denmark. *Geochimica et Cosmochimica Acta* **58** (23), 5115–5129.
- Thamdrup, B., Glud, R.N., Hansen, J.W., 1994b. Manganese oxidation and in-situ manganese fluxes from a coastal sediment. *Geochimica et Cosmochimica Acta* **58** (11), 2563–2570.
- Tebo, B.M., Bargar, J.R., Clement, B.G., Dick, G.J., Murray, K.J., Parker, D., Verity, R., Webb, S.M., 2004. Biogenic manganese oxides: properties and

- mechanisms of formation. *Annual Review of Earth and Planetary Sci.* **32**, 287-328.
- Tebo, B.M., Ghiorse, W.C., van Waasbergen, L.G., Siering, P.L., Caspi, R., 1997. Bacterially mediated mineral formation: insights into manganese(II) oxidation from molecular genetic and biochemical studies. In: *Geomicrobiology: Interactions Between Microbes and Minerals*. JF Banfield, KH Nealson, (Eds), Washington, DC. *Journal of the American Chemical Society*, 225–66.
- Trefry, J. and Presley, J., 1982. Manganese fluxes from the Mississippi Delta sediments. *Geochimica et Cosmochimica Acta* **46** (10), 1715–1726.
- Tebo, B.M., Bargar, J.R., Clement, B.G., Dick, G.J., Murray, K.J., Parker, D., Verity, R., Webb, S.M., 2004. Biogenic manganese oxides: properties and mechanisms of formation. *Annual Review of Earth and Planetary Sci.* **32**, 287-328.
- Van der Weijden, C.H., 1975. Sorption Experiments Relevant to the Geochemistry of Manganese Nodules. Ph.D. dissertation. University of Utrecht. 154 pp.
- van der Zee, C., van Raaphorst, W., Epping, E., 2001. Absorbed Mn^{2+} and Mn redox cycling in Iberian continental margin sediments (northeast Atlantic Ocean). *Journal of Marine Research* **59** (1), 133–166.
- Yeats, P. A., Sundby, B., Bowers, J. M., 1979. Manganese recycling in coastal waters. *Marine Chemistry* **8**, 43-55.

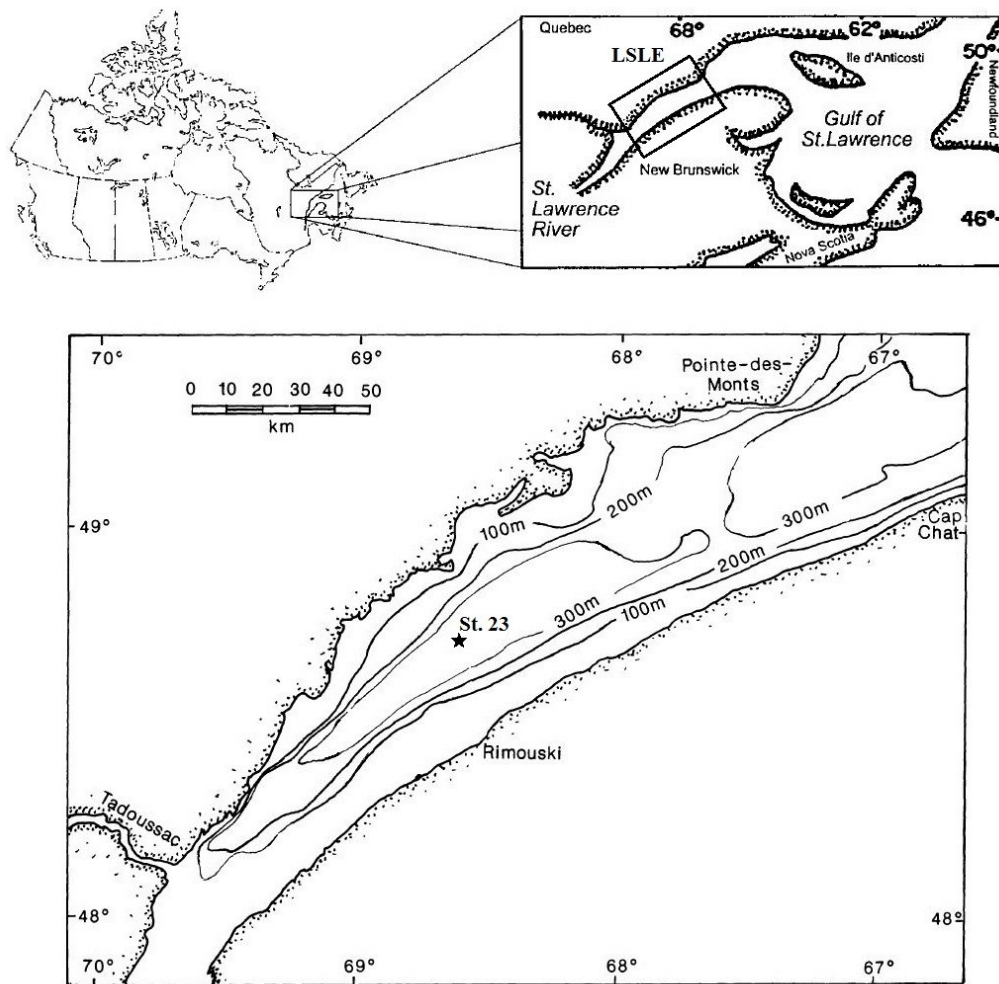


Figure 2.1 – Map of the Lower St. Lawrence Estuary showing the position of Station 23.

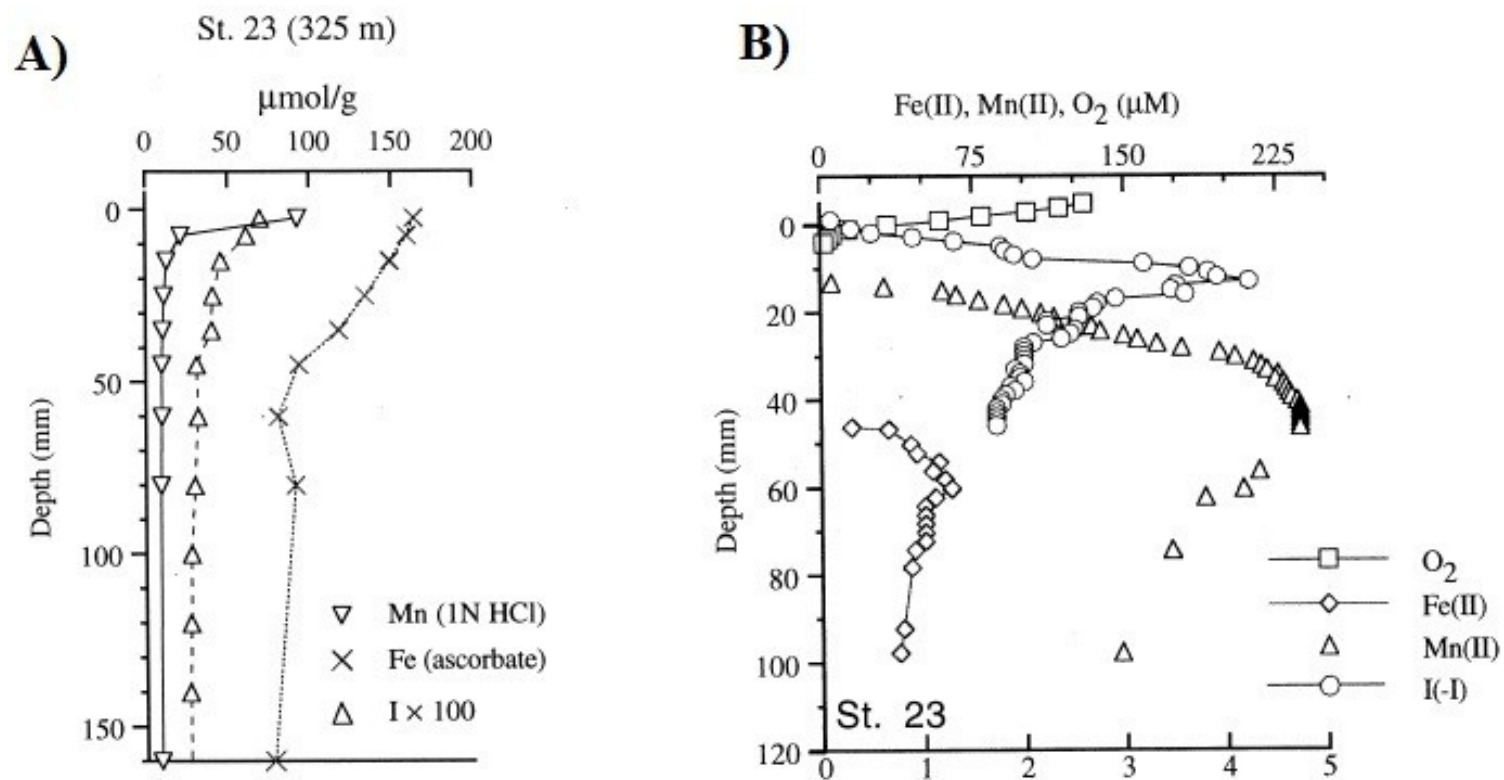


Figure 2.2 – A) Vertical distributions of reactive particulate Mn and Fe ($\mu\text{mol/g}$ dry wt.) and total I ($100 \times \mu\text{mol/g}$ dry wt.) at Station 23. B) Vertical distributions of dissolved O_2 , I(-I), Mn(II) and Fe(II) in sediment porewaters at Station 23 in $\mu\text{mol/L}$. The profiles were acquired with a solid-state gold/mercury amalgam microelectrode (Brendel and Luther, 1995). The detection limits for O_2 , I(-I), Mn(II) and Fe(II) were $3 \mu\text{mol/L}$, $<0.2 \mu\text{mol/L}$, and $5 \mu\text{mol/L}$, respectively. Figures taken from Anschutz et al. (2000).

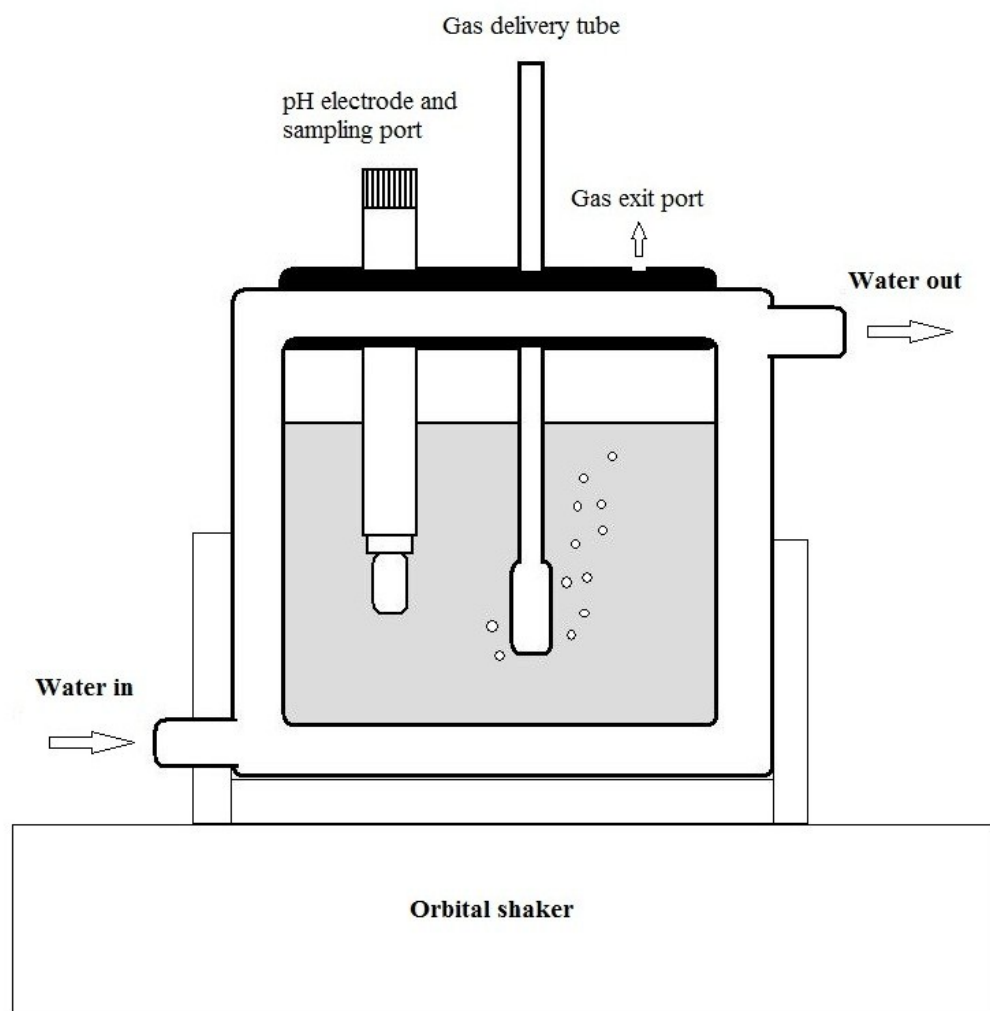


Figure 2.3 – Schematic representation of the experimental reactor.

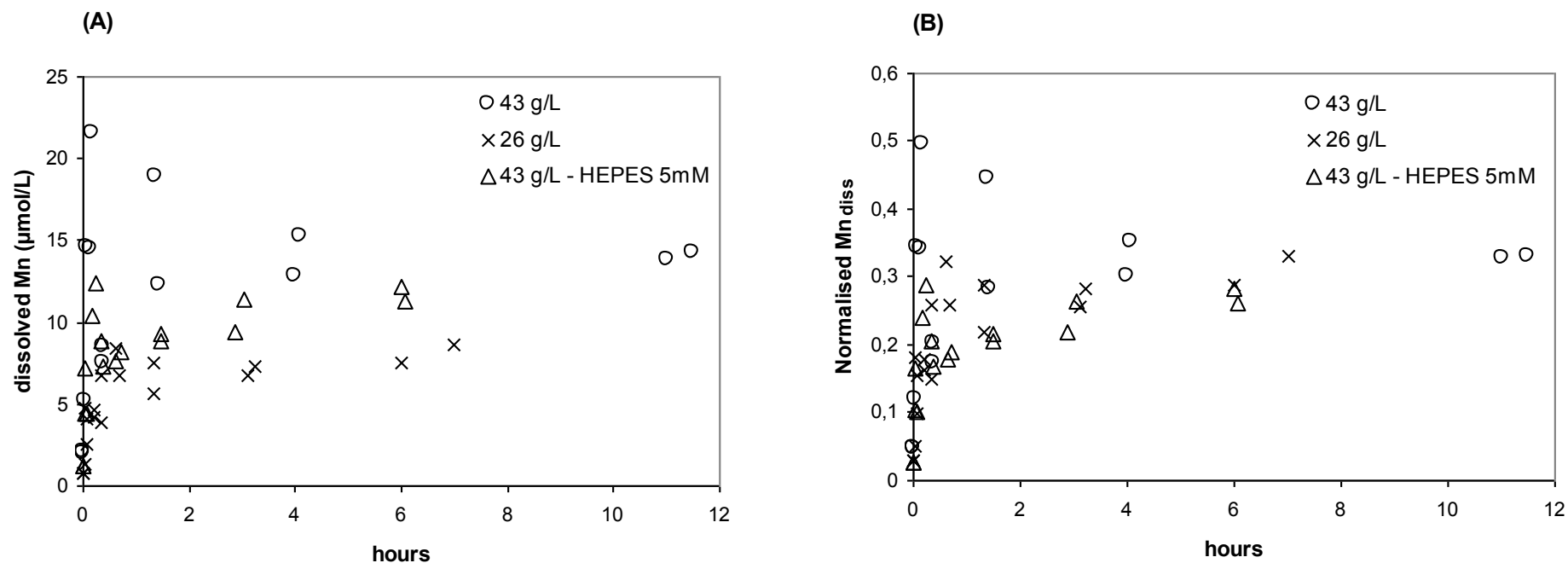


Figure 2.4 – Desorption experiments #4-5 (43 g/L), #8-9 (26 g/L) and #10-11 (43 g/L – HEPES 5 mM). Panel A shows the evolution of the dissolved Mn concentration during the course of the experiments. Panel B shows the temporal evolution of dissolved Mn concentration normalised to the dry weight of solid sediment. This ratio is obtained by dividing the concentration of dissolved Mn by the solid/solution ratio of the slurry and carries units of $\mu\text{mol g}^{-1}$ dry sediment.

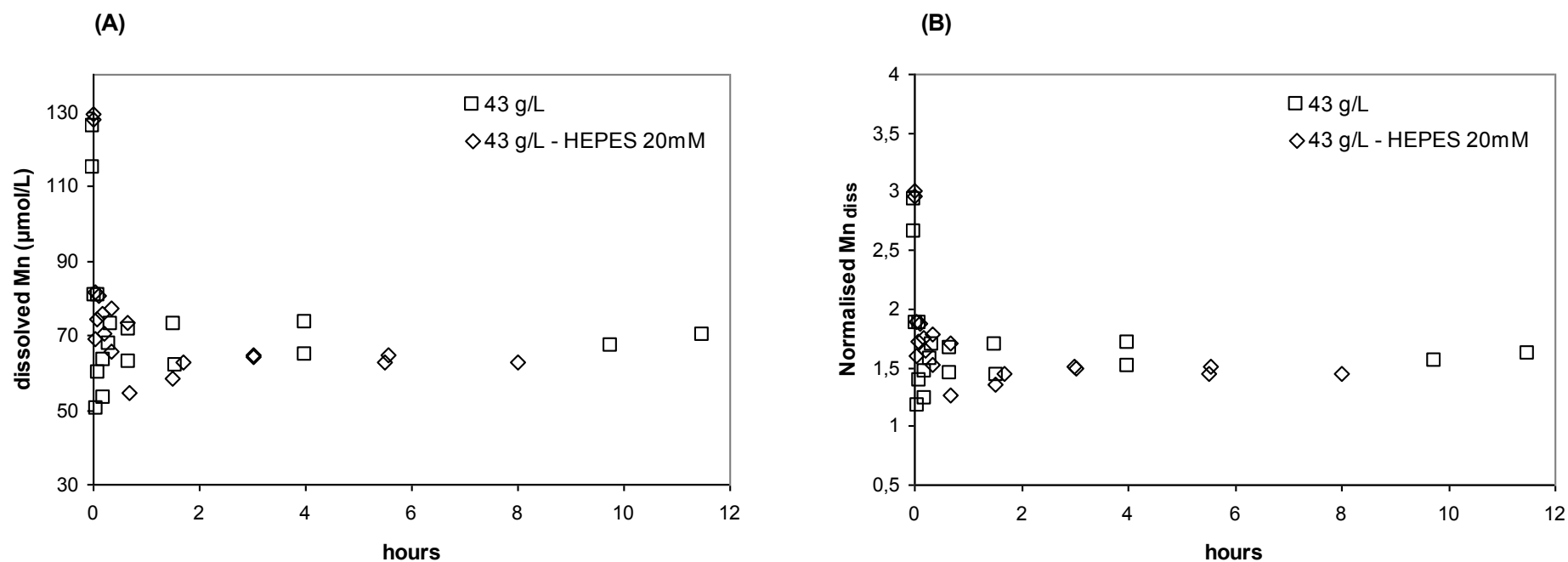


Figure 2.5 – Adsorption experiments #6-7 (43 g/L) and #12-13 (43 g/L – HEPES 20 mM). Panel A shows the evolution of the dissolved Mn concentration during the course of the experiments. Panel B shows the temporal evolution of dissolved Mn concentration normalised to the dry weight of solid sediment. This ratio is obtained by dividing the concentration of dissolved Mn by the solid/solution ratio of the slurry and carries units of $\mu\text{mol g}^{-1}$ dry sediment.

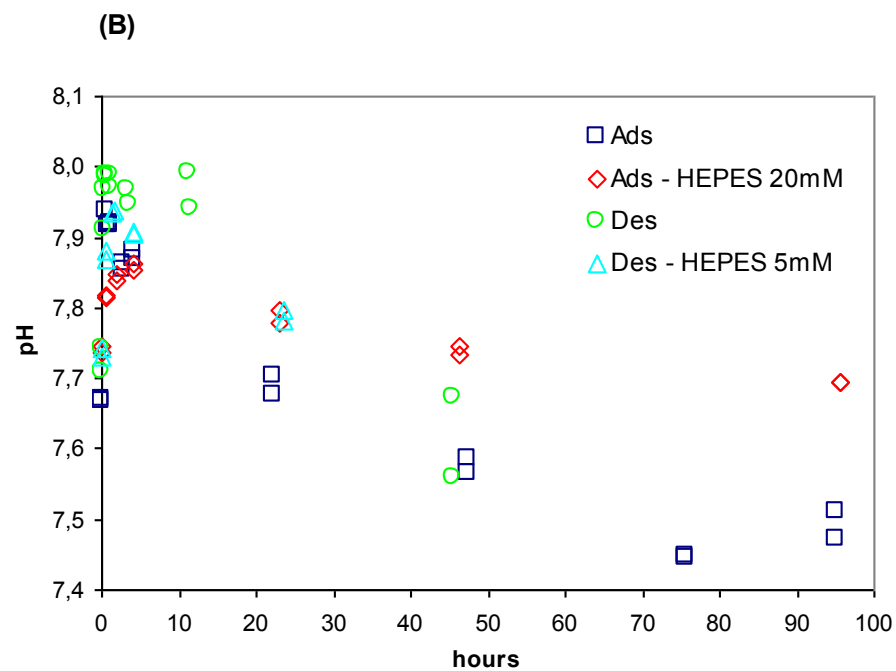
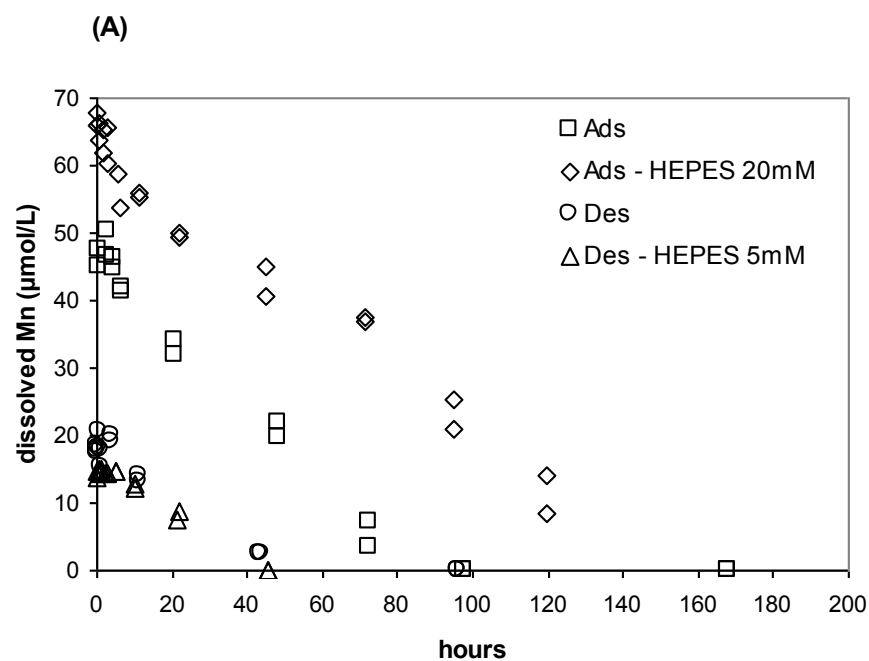


Figure 2.6 – Oxidation experiments #6-7 (Ads), #12-13 (Ads –HEPES 20 mM), #4-5 (Des) and #10-11 (Des – HEPES 5 mM). Panel A shows the evolution of the dissolved Mn concentration during the course of the experiments. Panel B show the temporal evolution of pH during the course of the experiments. The solid/solution ratio was 43 g/L for all experiments.

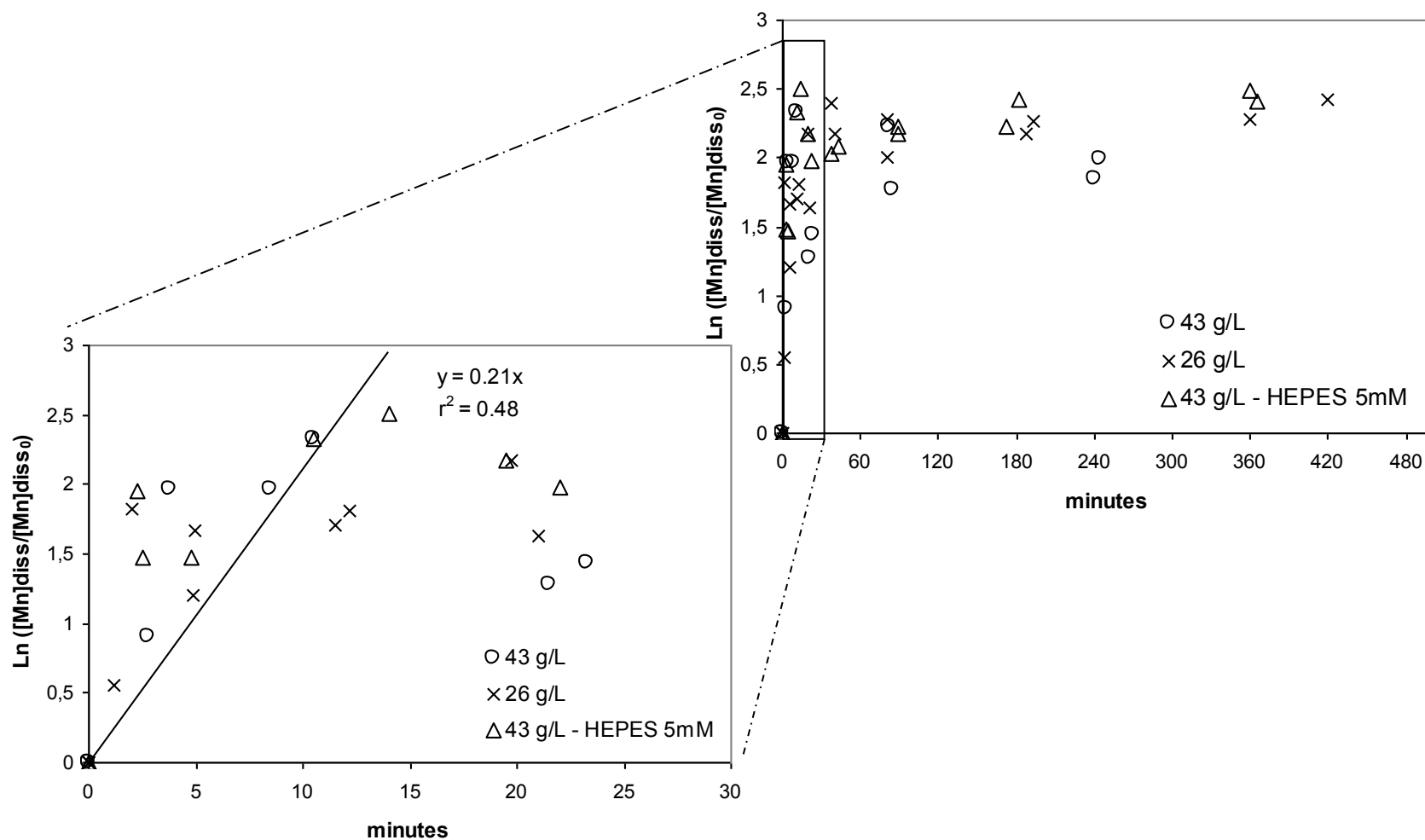


Figure 2.7 – First-order kinetics plot based on the time evolution of dissolved Mn concentrations in slurries during desorption experiments. The first-order rate constant $k_{des}' = 0.21 \pm 0.06 \text{ min}^{-1}$ was obtained from the slope of the regression line for the combined experiments #4-5 (43 g/L), #8-9 (26 g/L) and #10-11 (43 g/L – HEPES 5 mM). Only data obtained during the initial 15 minutes of each experiment were used to calculate the regression (see text for justification). The uncertainty on the least squares regression represents the 95% confidence interval.

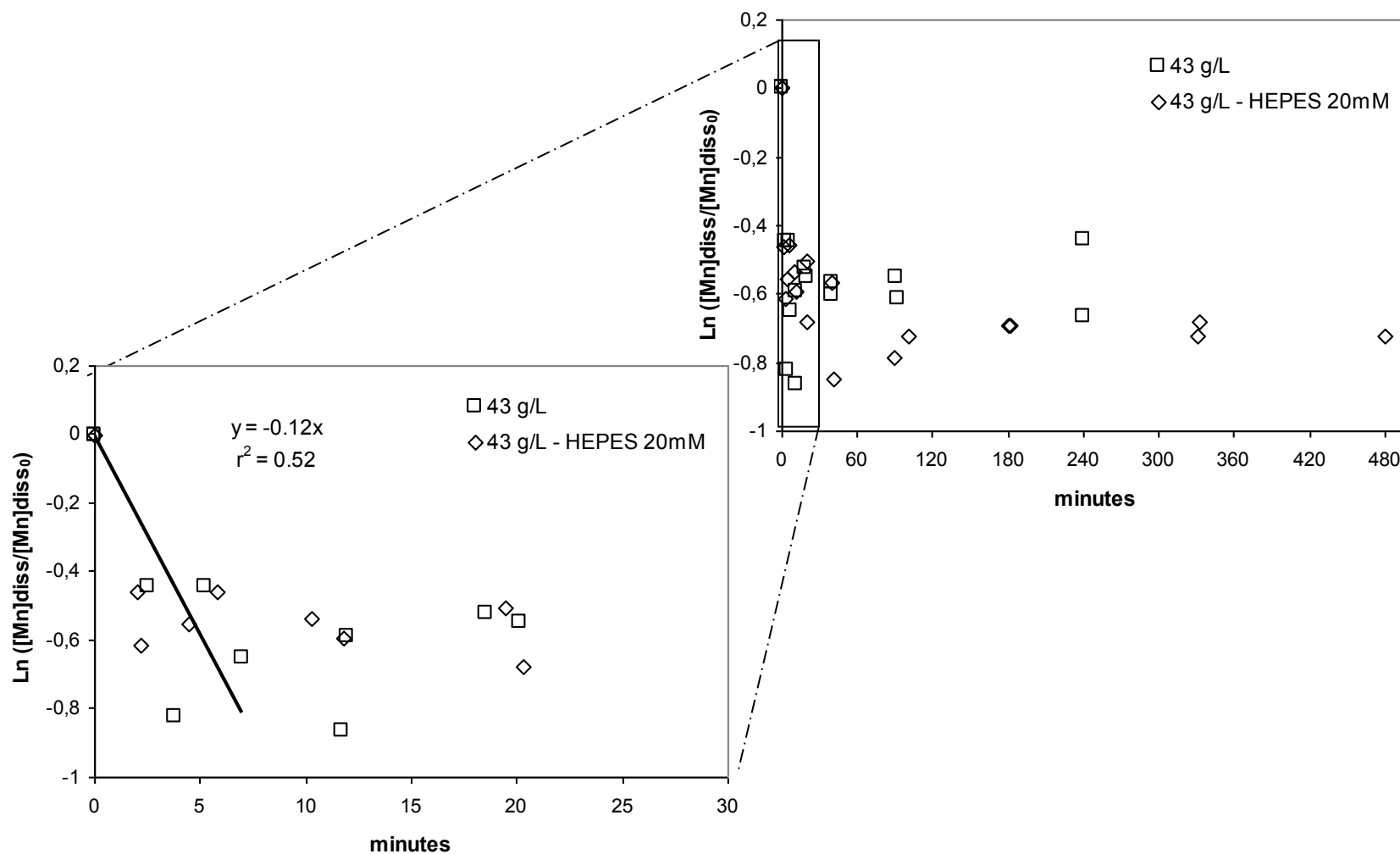


Figure 2.8 – First-order kinetics plot based on the time evolution of dissolved Mn concentrations in slurries during adsorption experiments. The first-order rate constant $k_{ads}' = 0.12 \pm 0.06 \text{ min}^{-1}$ was obtained from the slope of the regression line for the combined experiments #6-7 (43 g/L) and #12-13 (43 g/L – HEPES 20 mM). Only data obtained during the initial 7 minutes of each experiment were used to calculate the regression. The uncertainty on the least squares regression represents the 95% confidence interval.

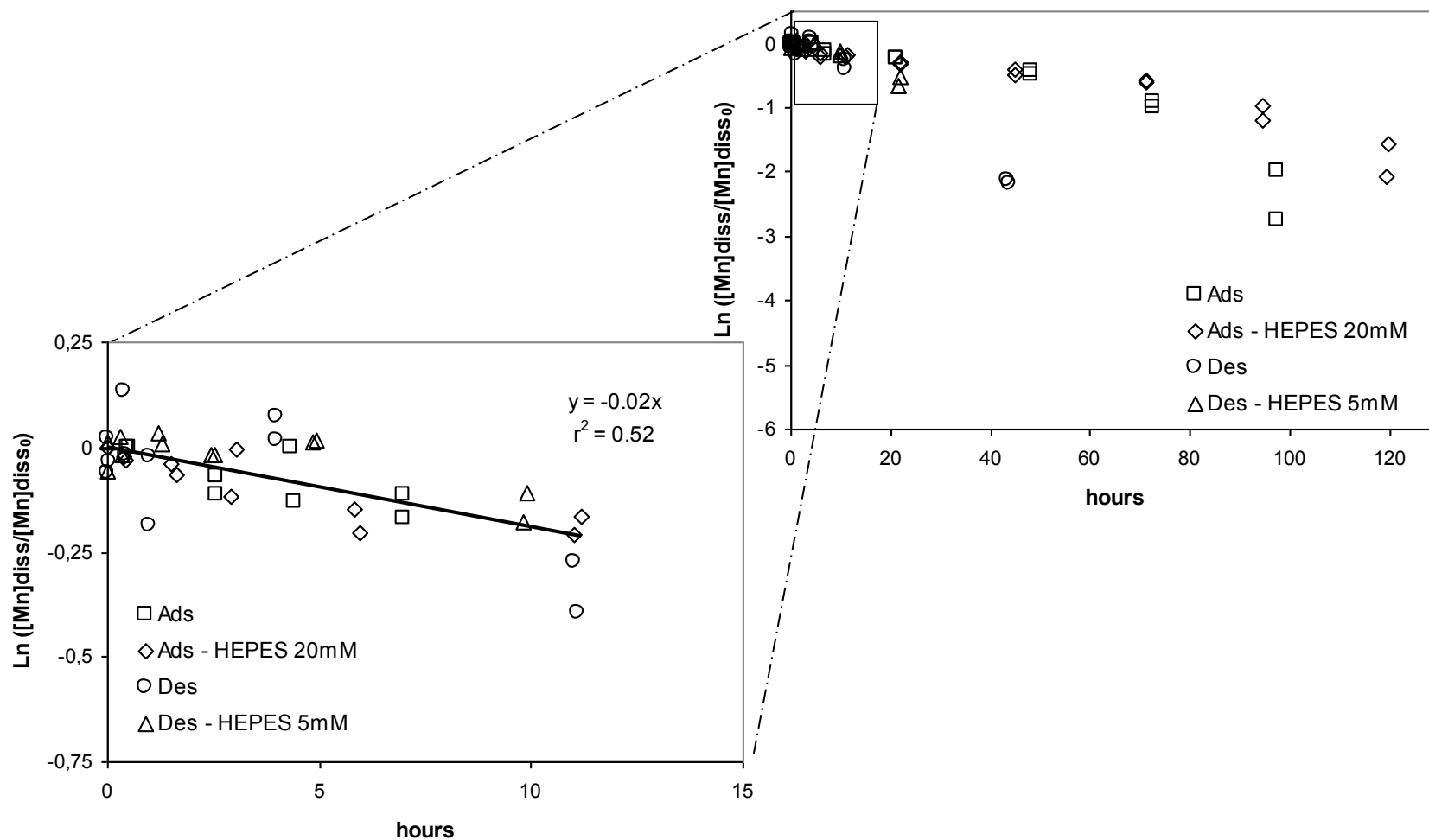


Figure 2.9 – First-order kinetics plot based on the time evolution of dissolved Mn concentrations in slurries during oxidation experiments. The pseudo-first-order rate constant $k_{ox}' = 0.020 \pm 0.006 \text{ hours}^{-1}$ was obtained from the slope of the regression line for the combined experiments #6-7 (Ads), #12-13 (Ads – HEPES 20 mM), #4-5 (Des) and #10-11 (Des – HEPES 5 mM). Only data obtained in the initial 12 hours of each experiment were used to calculate the regression. The uncertainty on the least squares regression represents the 95% confidence interval.

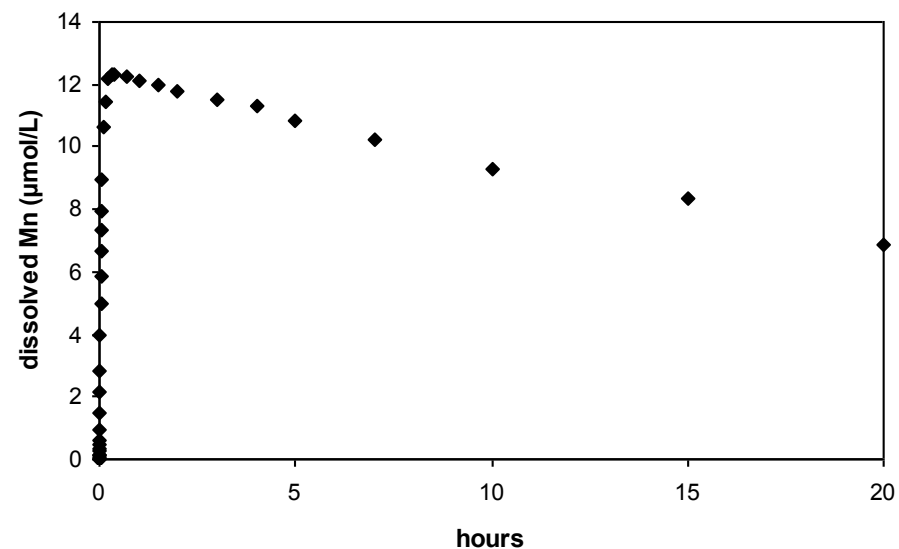


Figure 2.10 – Simulation of the hypothetical temporal evolution of dissolved Mn(II) from competing desorption and oxidation reactions upon exposure of anoxic sediments to oxygenated waters at 25°C and pH_{sws} = 7.7. In this simulation, $R = k_{des}' ([Mn_{diss}]_{ss} - [Mn_{diss}]) - k_{ox}' [Mn_{diss}]$ (see Eq. 3a and Eq. 4), for which the analytical solution is : $[Mn_{diss}]_t = ([Mn_{diss}]_{ss} (1 - e^{-k_{des}'t})) - e^{-k_{ox}'t}$. In this simulation $[Mn_{diss}]_{ss} = 12.5 \mu\text{mol/L}$ (the mean steady state value for desorption experiments #4-5 and #10-11 at a solid:solution ratio of 43 g/L).

Table 2.1 - Characteristics of homogenised sediment recovered at Station -23 in July 2009

Depth cm	Porosity	Mn _{HCl} ($\mu\text{mol/g}$ dry weight)
10-30	0.776 \pm 0.001	7.8

Table 2.2 - Characteristics and quantity of seawater and sediment used for the slurry incubation experiments

Experiment No	Initial Volume of seawater (mL)	Initial [Mn] _{diss} ($\mu\text{mol/L}$)	[HEPES] buffer ($\mu\text{mol/L}$)	Wet sediment weight (g)	[Mn] _{porewater} ($\mu\text{mol/L}$)	Total volume of seawater (mL)	Solid / solution ratio
4	285	<dl	0	30.269	37	302.0	43.4
5	285	<dl	0	29.501	37	301.5	42.4
6	285	110	0	30.000	28	301.6	43.1
7	285	105	0	30.000	28	301.6	43.1
8	291	<dl	0	18.100	23	301.0	26.0
9	291	<dl	0	18.100	23	301.0	26.0
10	285	<dl	0.005	30.000	21	301.6	43.1
11	285	<dl	0.005	30.000	21	301.6	43.1
12	285	130	0.02	30.000	21	301.6	43.1
13	285	130	0.02	30.000	21	301.6	43.1

Table 2.3 – Desorption experiments #4-5, #8-9 and #10-11

Sampling times (hours)	[Mn] _{diss} ($\mu\text{mol/L}$)	Normalised Mn _{diss} content ($\mu\text{mol/g dw}$)	pH _{SWS}
Experiment # 4 - desorption			
0	2.1	0.05	7.68
0.046	5.2	0.12	
0.175	22	0.50	
0.333			7.72
0.358	7.5	0.17	
0.667			7.72
1.4	12	0.28	
1.5			7.72
2.5			7.75
4.1	15	0.35	
4.3			7.75
11.5	14	0.33	
44	22	0.50	
48			7.71
95	17	0.40	
96			7.71
Experiment # 5 - desorption			
0	2	0.05	7.70
0.063	15	0.34	
0.142	15	0.34	
0.317			7.72
0.388	8.5	0.20	
0.667			7.73
1.4	19	0.45	
1.8			7.73
3.5			7.71
4	13	0.30	
11	14	0.33	
44	21	0.49	
48			7.71
95	18	0.44	

Sampling times (hours)	[Mn] _{diss} (μmol/L)	Normalised Mn _{diss} content (μmol/g dw)	pH _{sws}
Experiment # 8 - desorption			
0	0.8	0.03	
0.019	1.3	0.05	
0.083	4	0.16	
0.192	4.2	0.16	
0.329	6.7	0.26	
0.616	8.4	0.32	
1.3	7.5	0.29	
3.2	7.3	0.28	
7	8.6	0.33	
Experiment # 9 - desorption			
0	0.8	0.03	
0.033	4.7	0.18	
0.082	2.5	0.10	
0.203	4.7	0.18	
0.350	3.9	0.15	
0.667	6.7	0.26	
1.3	5.7	0.22	
3.1	6.7	0.26	
6	7.5	0.29	
Experiment # 10 - desorption			
0	1.2	0.03	
0.038	7.2	0.17	
0.233	12	0.29	
0.367	7.3	0.17	
0.533			7.69
0.713	8.2	0.19	
1.5	8.9	0.21	
2.8			7.75
3	11	0.27	
6	11	0.26	
24			7.74
25	13	0.32	

Sampling times (hours)	[Mn] _{diss} (μmol/L)	Normalised Mn _{diss} content (μmol/g dw)	pH _{sws}
Experiment # 11 - desorption			
0	1.2	0.03	
0.042	4.4	0.10	
0.079	4.4	0.10	
0.175	10.4	0.24	
0.325	8.9	0.21	
0.629	7.7	0.18	
1.5	9.3	0.22	
1.8			7.74
2.9	9.4	0.22	
6	12	0.28	
23			7.73
24	13	0.34	

Table 2.4 – Adsorption experiments #6-7 and #12-13

Sampling times (hours)	[Mn] _{diss} ($\mu\text{mol/L}$)	Normalised Mn _{diss} content ($\mu\text{mol/g dw}$)	pH _{SWS}
Experiment # 6 - adsorption			
0	115	2.66	7.65
0.063	50	1.17	
0.117	60	1.39	
0.2	63	1.47	
0.308	68	1.57	
0.375			7.67
0.663	63	1.45	
0.792			7.68
1.3			7.69
1.6	62	1.44	
3.4			7.72
4	74	1.71	
5			7.75
11.5	70	1.62	
25	60	1.39	
26			7.67
71	66	1.52	7.67
Experiment # 7 – adsorption			
0	130	2.93	7.67
0.042	81	1.88	
0.088	81	1.88	
0.195	53	1.23	
0.336	73	1.69	
0.408			7.67
0.663	71	1.66	
1.5			7.70
1.5	73	1.69	
3			7.71
4	65	1.50	
9.8	67	1.55	
24	74	1.72	

Sampling times (hours)	[Mn] _{diss} ($\mu\text{mol/L}$)	Normalised Mn _{diss} content ($\mu\text{mol/g dw}$)	pH _{SWS}
25			7.67
67			7.67
69	73	1.69	
Experiment # 12 - adsorption			
0	130	3.00	
0.033	82	1.89	
0.075	74	1.72	
0.172	76	1.76	
0.339	66	1.52	
0.517			7.72
0.658	74	1.71	
1.7	63	1.45	
3	65	1.50	
3.7			7.74
5.5	63	1.45	
8	63	1.45	
23			7.75
24	60	1.40	
Experiment # 13 - adsorption			
0	130	3.00	
0.036	69	1.61	
0.097	81	1.88	
0.197	71	1.64	
0.325	77	1.79	
0.679	55	1.27	
1.5	58	1.35	
1.8			7.74
3	64	1.49	
5.6	65	1.50	
22	63	1.45	7.74

Table 2.5 – Oxidation experiments #4-5, #6-7, #10-11 and #12-13

Sampling times (hours)	[Mn] _{diss} ($\mu\text{mol/L}$)	Normalised Mn _{diss} content ($\mu\text{mol/g dw}$)	pH _{SWS}
Experiment # 4 - oxidation			
0	17	0.40	7.71
0.033	18	0.41	
0.15			7.91
0.417	18	0.42	
0.617			7.99
1	15	0.35	
1.2			7.97
3.5			7.95
4	19	0.44	
11	13	0.30	
11.5			7.94
44	2.4	0.05	
46			7.67
96	<dl		
Experiment # 5 - oxidation			
0	18	0.44	7.74
0.233			7.97
0.383	21	0.49	
0.6			7.99
1	18	0.42	
1.1			7.99
3.3			7.97
4	20	0.47	
11	14	0.33	
11.3			7.99
44	2.4	0.06	
45			7.56
96	<dl		
Experiment # 6 - oxidation			
0			7.67

Sampling times (hours)	[Mn] _{diss} (μmol/L)	Normalised Mn _{diss} content (μmol/g dw)	pH _{SWS}
0.48	51	1.19	
0.683			7.94
1.133			7.92
2.583	45	1.04	
2.833			7.85
4			7.87
4.3	50	1.17	
7	46	1.07	
21	41	0.96	
22			7.68
48			7.57
48	32	0.74	
73	22	0.51	
76			7.45
95			7.47
98	7.2	0.17	
168	<dl		
Experiment # 7- oxidation			
0			7.67
0.533	53	1.23	
0.717			7.92
1.133			7.92
2.583	47	1.10	
2.833			7.86
4			7.88
4.4	47	1.08	
7	45	1.04	
21	42	0.97	
22			7.70
48			7.59
48	34	0.79	
73	20	0.46	
76			7.44
95			7.51

Sampling times (hours)	[Mn] _{diss} ($\mu\text{mol/L}$)	Normalised Mn _{diss} content ($\mu\text{mol/g dw}$)	pH _{SWS}
98	3.4	0.08	
168	<dl		
Experiment # 10 - oxidation			
0	14	0.32	7.74
0.317	15	0.35	
0.617			7.88
1.2	15	0.35	
1.5			7.94
2.5	14	0.33	
4.1			7.91
4.8	15	0.34	
9.8	12	0.28	
22	7.6	0.18	
24			7.80
45	<dl		
Experiment # 11 - oxidation			
0	15	0.34	7.73
0.35	14	0.33	
0.65			7.87
1.3	15	0.34	
1.6			7.94
2.6	14	0.33	
4.2			7.91
4.9	15	0.34	
9.9	13	0.30	
22	8.7	0.20	
24			7.78
45	<dl		
Experiment # 12 - oxidation			
0	68	1.58	7.75
0.4	66	1.54	
0.617			7.82
1.5	65	1.52	

Sampling times (hours)	[Mn] _{diss} (μmol/L)	Normalised Mn _{diss} content (μmol/g dw)	pH _{SWS}
1.8			7.85
2.9	60	1.40	
4			7.86
5.8	59	1.36	
11	55	1.28	
22	50	1.16	
23			7.80
45	45	1.04	
46			7.75
71	37	0.85	
95	21	0.48	
96			7.70
120	8.6	0.20	
Experiment # 13 - oxidation			
0	66	1.53	7.74
0.438	64	1.48	
0.667			7.81
1.6	62	1.43	
1.833			7.84
3	66	1.52	
4			7.85
6	54	1.25	
11	56	1.30	
22	49	1.14	
23			7.78
45	41	0.94	
46			7.73
71	37	0.87	
95	25	0.59	
96			7.69
120	14	0.32	

Table 2.6 – Compilation of the Mn(II) first-order oxidation rate constants taken from the literature and measured in this study

Sediment	First-order rate constant (year ⁻¹)	Reference
Coastal, Aarhus Bay	365	Calculated from the work of Thamdrup et al. (1994b)
Pelagic, Eastern North Pacifica (MANOP)	50	Dhakar and Burdige (1996)
Saguenay Fjord	10 ⁶	Mucci et al. (2003)
Coastal, Gulf of St. Lawrence	5 x 10 ⁵	Gratton et al. (1990)
Coastal, Lower St. Lawrence Estuary	2.4 x 10 ³ to 4.4 x 10 ⁵	Edenborn et al. (1985)
Coastal, Lower St. Lawrence Estuary	96	This study

Chapter 3. Final remarks

3.1 Research summary and conclusions

Mass balance calculations reveal that, in many coastal environments, the bottom sediments do not retain all the manganese that is delivered to the seafloor by settling particulate matter. Hence, there must be a net flux of dissolved manganese from the sediment back to the overlying water column (Sundby *et al.*, 1981; Trefry and Presley, 1982). Several processes have been proposed to account for this flux: diffusion of dissolved manganese across the sediment-water interface (McCaffrey *et al.*, 1980), release of manganese to the overlying water during migrations of the Mn(II)/Mn(IV) redox boundary towards the sediment surface (Sundby, 2006), and advection of anoxic sediment and pore fluid to the sediment surface (Schink and Guinasso, 1978; McCaffrey *et al.*, 1980; Saulnier and Mucci, 2000). The objective of this project was to evaluate if advection of anoxic sediment to the sediment-water interface, followed by desorption of dissolved Mn(II) from the exposed particles to the water column is an efficient process that supports a net flux of manganese from the sediment to the water column. To meet this objective, I determined the relative rates of desorption and oxidation of Mn(II) sorbed onto natural, anoxic sediments upon exposure to oxygenated seawater.

To determine the relative rates of Mn(II) adsorption, desorption, and oxidation, I conducted slurry incubation experiments by mixing natural anoxic sediment and bottom water from the LSLE. The experimental design allowed me

to conduct separate adsorption, desorption, and oxidation experiments. In these experiments, dissolved manganese concentrations were monitored over time, and the results obtained were used to derive first-order rate constants for each reaction. The first-order rate constants for Mn(II) adsorption, desorption, and oxidation in anoxic marine sediment indicate that adsorption and desorption are much faster than the homogeneous oxidation. Mn(II) is desorbed from anoxic sediment particles exposed to oxygenated bottom seawater on time scales of minutes, but homogeneous oxidation takes several hours. In natural aquatic environments, manganese can therefore be released from recently advected reducing sediment before it is oxidised and immobilised at the sediment surface.

3.2 Final remarks and recommendations

The slurry incubation experiments were designed to simulate a natural process: the exposure of anoxic Mn(II)-laden sediment to an oxygen-containing water column. Obviously, there are significant differences between our laboratory simulations and natural conditions in the LSLE, such as, the mode of resuspension, the temperature, the pressure, and, in some cases, pH and pO₂. Whereas some dissimilarities are inevitable, modifications to the experimental protocol would allow a more realistic simulation of the *in-situ* conditions.

The anoxic wet sediment I used in the slurry incubation experiments was stored at 4°C for over one year before being homogenised and transferred to the anaerobic chamber (see section 2.3.3). Perhaps because of this, the porewater

manganese concentrations of these anoxic wet sediment (see Table 2.2) were more than three times lower than those measured 10 cm below the sediment-water interface with a voltammetric micro-electrode by Anschutz *et al.* (2000). Furthermore, over the period of several months during which the sediment was stored in the anaerobic chamber, the porewater manganese concentrations gradually decreased. To better reproduce the conditions encountered in the natural environment, fresh anoxic sediments should be used in future experiments. Further modifications to the experimental design (see section 2.3.5) should also be considered in future experiments. Larger volume reaction vessels would allow the use of an increased speed of the orbital shaker and thus a more efficient resuspension of sediment particles. In our slurry incubation experiments, the heavier sediment particles were not completely resuspended at 160 RPM. The use of an ultrasonic bath could also help for the dispersion of particles at the early stage of resuspension experiments. In Future experiments, the influence of temperature, oxygen concentration, pH and other environmental variables on the reaction rates could be investigated. In addition, during Mn(II) oxidation experiments, the influence of surface catalysis processes and bacterial mediation could be evaluated by introducing manganese and iron oxides and by using bacterial poisons that do not interfere with the abiotic Mn(II) oxidation, such as mercuric chloride (Edenborn *et al.*, 1985). Finally, the second-order rate constant for heterogeneous Mn(II) oxidation could be determined.

3.3 Future work

The objective of this thesis was to estimate the relative rates of desorption and oxidation of Mn(II) sorbed to natural anoxic sediment upon exposure to oxygenated seawater and thereby evaluate the efficiency of advection of anoxic sediment particles as a mechanism for releasing dissolved manganese from the sediment to the overlying water. This objective was met and, based on the measured first-order desorption and oxidation rates, I concluded that advection of anoxic sediment to the sediment surface does indeed release Mn(II) to the water column. The significance of this process relative to other processes that may release dissolved manganese from bottom sediment (e.g. diagenetic remobilization, bioturbation rate) cannot be evaluated without additional information such as a quantitative estimate of the sediment reworking rate. The latter is defined as the advective flux, per unit surface area and time, of anoxic sediment particles to the oxidizing surface of the sediment column. This information is not available for LSLE sediments. Hence, future work should be directed towards estimating these rates. Although it is difficult to measure such rates in-situ, they could be measured experimentally by using sediment benthocosms using such methods as described by Rhoads (1967) and Kudenov (1982) who measured reworking rates of shallow or intertidal sediments by different species of polychaetes.

Finally, the rate of homogeneous Mn(II) oxidation we obtained in this study could be validated based on time-lapse colour photography of sediment mounds at the seafloor. Ultimately, if this rate can be linked to the color change

associated with the oxidation of reducing sediment, it could be used to estimate the frequency of anoxic sediment remobilisation by burrowing organisms.

3.4 References

- Anschutz, P., Sundby, B., Lefrançois, L., Luther III, G.W., Mucci, A., 2000. Interactions between metal oxides and species of nitrogen and iodine in bioturbated marine sediments. *Geochimica et Cosmochimica Acta* **64** (16), 2751–2763.
- Edenborn, H.M., Paquin, Y., Chateauneuf, G., 1985. Bacterial contribution to manganese oxidation in a deep coastal sediment. *Estuarine, Coastal and Shelf Science* **21**, 801-815.
- Kudenov, J.D., 1982. Rates of seasonal sediment reworking in *Axiiothella rubrocinta* (Polychaeta: Maldanidae). *Marine Biology* **70**, 181-186.
- McCaffrey, R.J., Myers, A.C., Davey, E., Morrison, G., Bender, M., Luedtke, N., Cullen, D., Froelich, P., Klinkhammer, G., 1980. The relation between pore water chemistry and benthic fluxes of nutrients and manganese in Narragansett Bay. *Limnology and Oceanography* **25** (1), 31-44.
- Rhoads, D. C., 1967. Biogenic reworking of intertidal and subtidal sediments in Barnstable Harbor and Buzzards Bay. *The Journal of Geology* **75**, 461-476.
- Saulnier, I. and Mucci, A., 2000. Trace metal remobilization following the resuspension of estuarine sediments: Saguenay Fjord, Canada. *Applied Geochemistry* **15**, 203–222.
- Schink, D. R. and Guinasso, N. L., 1978. Redistribution of dissolved and adsorbed materials in abyssal marine sediments undergoing biological stirring. *American Journal of Science* **278**, 687-702.

- Sundby, B., 2006. Transient state diagenesis in continental margin muds. *Marine Chemistry* **102**, 2-12.
- Sundby, B., Silverberg, N., Chesselet, R., 1981. Pathways of manganese in an open estuarine system. *Geochimica et Cosmochimica Acta* **45** (3), 293–307.
- Trefry, J. and Presley, J., 1982. Manganese fluxes from the Mississippi Delta sediments. *Geochimica et Cosmochimica Acta* **46** (10), 1715–1726.